Simulation of climatic change due to increased atmospheric CO_2

by

J.F.B.Mitchell

DCTN 39

April 1986

DYNAMICAL CLIMATOLOGY TECHNICAL NOTE NO. 39

SIMULATION OF CLIMATE CHANGE DUE TO INCREASED ATMOSPHERIC CO_2

by

J F B Mitchell

Notes for NATO Advanced Study Institute on "Physically-based modelling and simulation of climate and climatic change", Erice, Sicily, 11-23 May 1986.

Met O 20 (Dynamical Climatology Branch)
Meteorological Office
London Road
Bracknell
Berkshire, England RG12 2SZ

April 1986

Note: This paper has not been published. Permission to quote from it should be obtained from the Assistant Director of the above Meteorological Office Branch.

LF/M020

SIMULATION OF CLIMATE CHANGE DUE TO INCREASED ATMOSPHERIC CO_2

by J F B Mitchell

Meteorological Office, Bracknell, Berkshire RG12 2SZ, ENGLAND

1. Introduction

The concentration of atmospheric CO_2 is, to a first approximation, well mixed throughout the troposphere and lower stratosphere. Measurements made at Mauna Loa indicate the concentration of atmospheric CO_2 has risen from 316 ppmv in 1958 to 342 ppmv in 1985 (Figure 1, from Trabalka, 1985), and was probably about 300 ppmv at the turn of the century (see Oeschger and Stauffer, 1986). This change is attributed mainly to the increased emission from fossil fuels (Figure 2). It has been estimated that the concentration of atmospheric CO_2 could exceed 600 ppmv by the end of the next century, but this estimate is subject to the uncertainties in forecasting the future use of fossil fuels, and predicting the response of the natural carbon cycle. These topics are considered further in a recent review edited by Trabalka (1985) and references therein. A comprehensive assessment of the natural carbon cycle is given by Bolin et al (1979).

The possibility that artificially produced CO_2 might affect climate was first considered by Callendar (1938). Over the last 15 years, the advent of numerical models of climate and confirmation of the accelerating increase in observed CO_2 concentrations has stimulated widespread interest

in 'the CO_2 problem'. This is reflected in the number of recent review articles, for example, US National Research Council (1979, 1982, 1983), Clarke (1982), Bach et al (1983), Liss and Crane (1983), US Department of Energy (1985a, b, c, d) and WMO/ICSU/UNEP (1985). The modelling of the climatic effects of CO_2 has been pioneered by Manabe and colleagues at the Geophysical Fluid Dynamics laboratory in Princeton (GFDL) and much of that work has been reviewed recently (Manabe, 1983).

In this chapter, the emphasis will be on the understanding of the physical mechanisms relevant to CO_2 induced climate change as the state of the art is not yet adequate to make detailed quantitative predictions of climate change. In doing so, I have attempted to refer to typical results, rather than trying to give a comprehensive review of numerical studies of the effect of increased CO_2 on climate. (A more detailed survey of recent work is given in Schlesinger and Mitchell, 1985).

We will be mainly concerned with the effects of enhanced CO_2 from the beginning of the industrial revolution (about 100 years ago) until the end of the next century. In other words, we are interested in time scales of up to a few centuries at most. We define a thermal response time to be the e-folding time to equilibrium (ie the time taken to reach 63% of the equilibrium temperature change due to a change in thermal forcing). As can be seen from Table 1, the thermal response times of the atmosphere, and surface and upper ocean lie well within this time scale, and that of the deep ocean partly so, hence these systems must be represented in our

numerical models. On the other hand, the continental ice sheets have a much longer thermal response time, and hence it is assumed that on the time scale of interest, they will remain substantially unchanged.

The remainder of this paper is laid out as follows. In the next section, the basic physics of the problem is presented, and some important feedback processes are discussed using results from one-dimensional models. In section 3, studies using three-dimensional models are discussed and assessed, including the early GFDL 'swamp' model experiments, more recent studies using realistic geography and a full seasonal cycle, and some preliminary studies using a simplified coupled dynamical ocean-atmosphere model. For completeness, a brief discussion of the problem of detecting changes in climate due to enhanced CO_2 concentrations is included. In the final section, the main findings from numerical studies to date are summarized, and priorities for future research are discussed.

2. Radiative forcing and simple feedback mechanisms

2.1 Radiative effects

The earth/atmosphere system is heated at a rate $(1-\alpha)S_o/4$ by solar (short wave) radiation, where S_o is the solar constant, α is the fraction of radiation reflected by the earth and atmosphere, currently about .33, and the factor of 4 allows for the spherical shape of the earth. This must be balanced by longwave (thermal or infra-red) cooling to space. For a perfect emitter, for example the earth's surface or thick cloud, the rate of longwave cooling is given by σT^4,

where T is the temperature of emitter, and σ is Stefan's constant. If the earth had no atmosphere, and α were unchanged, the surface temperature of the earth T would be given by

$$\frac{S_o}{4}(1-\alpha) = \sigma T^4 \qquad (1)$$

or approximately 255 K (-18°C). Certain gases (water vapour, carbon dioxide, ozone) absorb solar radiation weakly, but strongly absorb and emit longwave radiation. The (increased) downward longwave radiation from these gases is responsible for the earth's surface temperature being 288 K (15°C), some 33 K warmer than expected according to equation (1), a phenomenon often referred to as the 'greenhouse' effect.

Most of the radiation emitted to space emanates from the atmospheric gases rather than the surface. The effective emitting temperature of 255 K given by equation (1) corresponds to a height of about 6 kilometres. By increasing the concentration of an atmospheric absorber such as CO_2, the mean level from which radiation escapes to space moves to a higher, and therefore colder, level (see Figure 3). The longwave cooling to space is reduced and the earth/atmosphere system warms until the longwave cooling again balances the incoming solar radiation.

In order to model the climatic effects of increasing atmospheric CO_2 concentrations, the radiative perturbation must be represented accurately. This depends on the correct representation of the radiative properties both of CO_2 and of other absorbers which are

active at the same wavelengths. Radiatively active constituents absorb and emit radiation at the same wavelengths. The spectral distribution of longwave radiation emitted by the atmosphere and reaching the surface under a typical vertical profile of temperature and gaseous absorbers is shown schematically in Figure 4 (dashed line). The solid line denotes the upward flux from the surface.

The main absorption (and emission) by CO_2 is due to transitions from the ground state in the 15 μm region. Weaker absorption occurs due to transitions from the first excited state in the region 12-18 μm and 10 μm ('hot' bands) and a pressure induced fundamental band near 7.6 μm (Augustsson and Ramanathan, 1977). Water vapour also absorbs strongly near 15 μm and thus reduces the absorption by CO_2 at those wavelengths, whereas the 7.6 μm and 10 μm bands are in the atmospheric 'window' where there is little other atmospheric absorption and emission, (Figure 4) and so are relatively more effective in trapping outgoing longwave radiation. In addition to absorption by the rotational bands of water vapour noted above, 'continuum' absorption due to water vapour over both the atmospheric window and the 12-18 μm region must be taken into account. A recent assessment of the accuracy of longwave radiation codes has been made by Luther and Fouquart (1984).

On doubling CO_2 from 320 ppmv, the globally averaged net downward flux of longwave radiation at the tropopause is enhanced by about 4 Wm^{-2} due to radiative effects alone (Kiehl and Ramanathan, 1982). From equation (1), this would produce a warming of 1.1 K in the absence of any feedback. Note that most of the enhanced flux is absorbed within the troposphere and only a small fraction reaches the surface, especially in the tropics where reabsorption due to water vapour is high. (The absorption of solar radiation in the atmosphere is enhanced by about 1 Wm^{-2}, but this is largely compensated by reduced absorption at the surface).

2.2 Radiative convective models

The global mean temperature in the upper atmosphere (stratosphere) is close to radiative equilibrium, but this is not true in the lower atmosphere (troposphere). If the temperature in the troposphere was controlled by radiation alone, the decrease in temperature with height (or lapse rate) would be much greater than observed (Manabe and Wetherald, 1967). The density of air increases with increase in pressure and decreases with increase in temperature. In regions where dense air overlies less dense air, the atmosphere produces overturning (mixing in the vertical, or convection) until the lapse rate is reduced to the stable value, which is 9.8 K/km for dry air. If moisture is present, rising air may cool sufficiently to become supersaturated, so that condensation occurs and latent heat is released. This further reduces the lapse rate, so the global mean value is about 6.5 K/km. To summarise, the equilibrium temperature of

the troposphere is dependent on the balance between radiative cooling to space and the convective transfer of heat from the surface. Conversely, the surface is heated radiatively, and cooled by the loss of sensible and latent heat to the atmosphere. Both these processes must be represented in any model which is to be used to study the surface and tropospheric response to increased CO_2.

In a radiative convective model, the vertical profile of temperature and atmospheric absorbers is represented at a number of levels in the vertical, and may be representative of annual mean conditions, or those pertaining to a particular latitude and season. (See earlier chapters by Fouquart, Ramanathan and Schlesinger). The radiative heating rates are calculated from the discretised equations of radiative transfer for both longwave and solar wavelengths, and the convective heating may be obtained by mixing heat between adjacent unstable layers to restore the global mean lapse rate (convective adjustment). In this case, the exchange of sensible and latent heat from the surface, and the vertical redistribution throughout the depth of the atmosphere are represented implicitly. In other models, the exchange of heat at the surface, its transfer in the vertical and the release of latent heat may be represented more explicitly. In particular, the convective adjustment procedure may be modified to allow for the exchange of air between non-adjacent layers in the vertical (penetrative convection) in order to represent the processes occurring in deep convective clouds.

In sensitivity experiments, the normal procedure is to run the model to equilibrium using present day and perturbed values of the model parameter (for example, CO_2 concentration) and to compare the results. These models are relatively cheap to run and easy to understand and have been used to explain the results found in more complex models. However, they omit many of the important components of the atmosphere, and, as will be seen, the results obtained are largely dependent on the assumptions made in the model. The examples presented here have been chosen because they clarify certain aspects of the general circulation model experiments discussed later.

2.3 Some climate feedbacks

Radiative convective models were first used by Manabe and Wetherald (1967) using global annual mean conditions and a critical lapse rate of 6.5 K/km. Increasing CO_2 produced a cooling of the model's stratosphere, and a warming of the troposphere. When the absolute humidity of the atmosphere was held constant, the surface temperature rose by 1.33 K which is in reasonable agreement with the value of 1.1 K based on pure radiative equilibrium calculated earlier (Manable and Wetherald (1975) report that a revised version of their radiation code is slightly less sensitive to enhanced CO_2). Observations of the seasonal variation of temperature and humidity indicate that relative humidity rather than absolute humidity is likely to be conserved. With constant relative humidity, Manabe and Wetherald found an increase of 2.36 K on doubling CO_2. With the revised radiation scheme, they obtain a value of 1.9 K, in close

agreement with Hansen et al (1981). Ramanathan (1981) and others have analysed the separate processes contributing to the change in surface temperature. An instantaneous increase in atmospheric CO_2 produces an increase in the radiative flux divergence in the stratosphere and hence a cooling and a decrease in the net upward long wave flux at the tropopause, warming the troposphere and surface. The troposphere warms, further enhancing the downward long wave flux at the surface. The surface warming would be expected to enhance evaporation, increasing the moisture content of the atmosphere, still further increasing the downward long wave flux at the surface. This last process, known as the 'water vapour feedback' is included implicitly in models which specify a fixed relative humidity, and increases rapidly with temperature.

In other studies (for example Rowntree and Walker, 1978, Lal and Ramanathan, 1984), surface and convective process are represented using the parametrizations taken from general circulation models, enabling a more direct representation of the water vapour feedback. If the release of latent heat in the atmosphere is taken into account explicitly (Rowntree and Walker, 1978) or implicitly (Hansen et al, 1981) in the convective adjustment scheme, much of the heating at the surface is converted to latent heat and released in the upper troposphere. The surface warming is reduced by about 40% and the warming in the upper troposphere is increased (Figure 5). This process is particularly important in the tropical atmosphere, where moist convection tends to adjust the vertical temperature gradient towards the moist adiabatic lapse rate. Since this lapse rate

decreases with increasing temperature, the warming due to increased CO_2 is enhanced at upper levels relative to that found with a constant lapse rate (Figure 5), but the surface warming is reduced. Conversely, where the atmospheric profile is more stable than average (as over the extratropical continents in winter) the surface warming will be enhanced. Manabe and Wetherald (1967) also investigated the effects of changes in cloud cover on surface temperature. Clouds reflect solar radiation to space, and so tend to cool the earth/atmosphere system. On the other hand, they absorb (and emit) longwave radiation. As cloud top height is increased, the cloud top temperature becomes progressively lower than the surface temperature, reducing the emission of longwave radiation from cloud top to space and thus enhancing the radiative heating of the troposphere and surface. Manabe and Wetherald found that for all but high cloud, the reduction in solar heating dominated the increase in longwave heating, but this result is dependent on the prescription of cloud reflectivities and emissivities, the incoming solar radiation and the albedo of the surface. Ohring and Clapp (1980) concluded on the basis of an observational study that clouds cool rather than warm the surface, though it should be noted that they made certain unverified assumptions in their analysis.

In their investigation of the effect of increased CO_2, Manabe and Wetherald (1967) assumed that the height of their cloud layers did not change when CO_2 was enhanced. In other studies (for example, Augustsson and Ramanathan, 1977; Hansen et al, 1981) the cloud top altitude was adjusted to keep the cloud top temperature constant.

Cloud top temperature controls the upward long wave radiation escaping to space from the cloud top. If cloud top altitude is fixed, the cloud top temperature is increased with enhanced CO_2, increasing the upward flux of long wave radiation and reducing the warming due to CO_2. If cloud top temperature is fixed, this negative feedback is removed and the sensitivity to CO_2 is enhanced. For example, Hansen et al (1981) found the sensitivity of surface temperature to doubling CO_2 increased by 40%.

It is possible that the increase in atmospheric water vapour predicted with enhanced CO_2 would be accompanied by an increase in cloud liquid water content. This in turn would change cloud optical properties and in particular, tend to increase the reflectivity of cloud (Stephens 1978). Somerville and Remer (1984) have attempted to quantify this feedback by deriving an empirical relationship between cloud liquid water content and atmospheric temperature using observational data from Feigelson (1973). Using this relationship in a radiative convective model, they find that the warming due to doubling CO_2 while maintaining constant relative humidity reduces the surface warming from 1.7 K to about 0.8 K. Hansen et al (1984) note a similar reduction in sensitivity assuming that cloud liquid water content is proportional to absolute humidity. Although these results may be qualitatively correct, cloud liquid water depends on factors other than temperature. Even in Feigelson's data, there is little change in cloud liquid water content with temperature at temperatures above 273K.

2.4 A cautionary tale

Attempts have been made to quantify the contribution to the change in surface temperature alone from the various processes including those described above, by considering the energy budget of the surface in isolation from the atmosphere (Idso 1980, Newell and Dopplick 1981). This approach can be very misleading since the temperature of the surface and troposphere are strongly coupled (Ramanathan 1981, Watts 1982). In principle, it is possible to perturb the tropospheric heating rates without initially altering the heating at the surface, and yet produce substantial warming at the surface at equilibrium. From an analysis of the surface heat budget, one would conclude that the feedback at the surface was infinite! Indeed, Kiehl and Ramanathan (1983) calculate that the instantaneous increase in radiative heating at the surface due to doubling CO_2 is only 0.55 Wm^{-2}. This would lead to a temperature rise of 0.1 K (at 288K) in the absence of feedbacks if the surface were in pure radiative equilibrium, in contrast to the increase of 1.1 K arrived at earlier by considering both the surface and troposphere. Any attempt to define a 'surface response function' (the ratio of the equilibrium surface temperature change to the initial change in radiative heating at the surface) will be futile, since the final surface temperature change will depend on the perturbation at both the surface and in the overlying atmosphere. The relative importance of the surface and atmospheric perturbations will, in turn, depend on the phenomenon considered.

2.5 Limitations of one-dimensional models

From the limited results above, it can be seen that the magnitude of the surface warming predicted by radiative convective models is largely dependent on the assumptions made in the model. In addition, many important processes affecting climate, such as horizontal advection of heat and moisture, and temperature/albedo feedbacks may be omitted entirely. They have, however proved a useful tool to explain the results from more complex models such as those discussed in Section 3. In particular, we will refer to the feedbacks due to water vapour, lapse rate, cloud distribution and cloud optical properties discussed above.

Before proceeding, it is useful to note that the change in surface temperature is approximately proportional to the logarithm of the change in CO_2 concentration, provided large increases of CO_2 are not considered (Augustsson and Ramanathan, 1977). This conclusion is supported by the computed changes in global mean surface temperatures in the three-dimensional studies described in the following section. In some of these studies a quadrupling rather than a doubling of CO_2 concentration is used in order that the response may be detected above the inherent variability of the model.

3. Equilibrium studies using general circulation models

3.1 Introduction

Many aspects of climate such as horizontal transport, land/sea contrasts and effects of orography are treated inadequately or omitted altogether in radiative convective models. Hence there has been an enormous effort to develop and use three-dimensional models of climate which will be described during the course of this Study Institute.

As noted in Section 1, atmospheric CO_2 and trace gases are increasing on a time scale of decades to centuries, and hence changes in ocean temperatures and sea-ice must be taken into account. Due to the large thermal inertia of the deep oceans, it has not been practical to integrate a detailed climate model with a deep ocean to equilibrium, though this is now possible if the seasonal cycle of solar radiation is ignored (see Bryan, this volume). Hence, most work to date has involved models with a grossly simplified representation of the ocean.

3.2 Early studies

In the earliest study (Manabe and Wetherald, 1975), oceanic heat storage and transport were ignored, and sea surface temperatures were determined diagnostically such that the net heat flux across the air-sea interface was zero. Sea-ice was predicted where the ocean temperature fell below the freezing point of sea water. This

representation of the ocean is often referred to as as 'swamp' ocean. The diurnal and seasonal variation of incoming solar radiation must be ignored in view of the neglect of the ocean's heat capacity. Manabe and Wetherald also limited the computational domain to a sector covering approximately one sixth of the globe, used an idealized land/sea distribution and ignored the effects of topography.

The simulated equilibrium change in atmospheric temperature due to doubling CO_2 (Figure 6) varies considerably with latitude. In low latitudes, the warming is about 2 K near the surface and increases to over 3 K at upper levels. As noted in section 2, in the tropical atmosphere the vertical gradient of temperature tends to the moist adiabatic lapse rate which becomes smaller as temperature increases, leading to enhanced warming at upper levels. Conversely, in high latitudes, the surface warming is enhanced because the inherent stable stratification inhibits the transfer of heat to upper levels. Two further mechanisms contribute to the enhanced surface warming in high latitudes. The increase in temperature will reduce the extent of highly reflective snow and sea-ice cover, leading to increased absorption of insolation and further warming (temperature/albedo feedback). Secondly, the atmospheric water content is greater in the warmer atmosphere, leading to a larger poleward transport of moisture and enhanced latent heat release in high latitudes. The areal mean warming on doubling CO_2, 2.9 K, is larger than the 2.4 K found using the equivalent radiative convective model (Table 2), due to the additional temperature/albedo feedback.

The net radiative heating of the surface increases by 3.4% due mainly to enhanced CO_2, and the increase in water vapour which accompanies the atmospheric warming. This enhanced radiative heating is balanced by a 7% increase in evaporation (and precipitation) and a small decrease in the upward flux of sensible heat. As the rate of change of the saturation vapour pressure with temperature is faster than linear, the ratio of the surface fluxes of latent heat to sensible heat increases with temperature where surface moisture is unlimited. Since the available incoming energy is limited, evaporation increases at the expense of the flux of sensible heat. Evaporation increased at all latitudes whereas precipitation increased mainly in high latitudes.

3.3 Detailed studies with prescribed cloud cover

The components of the atmospheric heat balance in Manabe and Wetherald's experiment changed only by a few percent on doubling CO_2. This is not surprising since the radiative perturbation at the top of the troposphere due to doubling CO_2 (4 Wm^{-2}) is small compared to the radiative cooling of the unperturbed atmosphere (typically 100 Wm^{-2}). It follows that the effect of increasing CO_2 may be regarded as a perturbation, and that the accurate simulation of the changes due to CO_2 requires a faithful simulation of present day climate. Some of the consequences of using an inadequate control simulation will be discussed later in this section.

The use of annually averaged incoming insolation leads to strong meridional temperature gradients which are more characteristic of winter than summer. Useful as Manabe and Wetherald's study is for illustrating some of the physical mechanisms which contribute to changes in climate, it gives no guidance on the seasonal and regional changes which, for example, are necessary for the assessment of the likely social and economic effects of increased CO_2. To do so, one must use a model which includes the annual cycle of insolation. This has been attempted using two differing but complementary approaches.

In the first approach, the ocean is represented by a static pool with the depth (typically 50 to 70 metres) chosen to provide reasonable simulation of the annual cycle of sea surface temperatures over most of the oceans. A simple representation of sea-ice is also included. This approach allows the sea surface temperatures and sea-ice extents to interact with the atmosphere as it responds to the increase in CO_2 concentrations. It has the disadvantage that errors in the atmospheric model, and the crudeness of the ocean model lead to errors in the simulation of present day climate which may distort the response of the model to small perturbations. For example, in the first such study (Manabe and Stouffer, 1980), the control simulation failed to reproduce the equatorial minimum in sea surface temperatures in the east Pacific and the winter sea-ice extents in the Arctic and Antarctic were respectively grossly over- and under-estimated.

Manabe and Stouffer (1980) investigated the effect of quadrupling CO_2 amounts in a model with realistic geography and orography, and using prescribed zonally averaged cloud cover. The global mean surface temperature increased by 4.1 K. In the tropics, warming is less than 3 K near the surface and increases to over 4 K in the upper troposphere, whereas in high latitudes in winter, especially over the Arctic, the warming is a maximum near the surface and decreases rapidly with height, in qualitative agreement with Manabe and Wetherald (1975). However, in high latitudes in summer, the lower atmosphere is not inherently stable in the unperturbed integration, and so the warming is more uniformly distributed in the troposphere. In the Arctic in summer, the near surface warming is small for reasons discussed later. In summary, the surface warming is a minimum in the tropics, where there is little seasonal variation (Figure 8) and in the Arctic in summer, and largest in high latitudes in autumn or winter.

In the 4 x CO_2 integration, the areal extent of highly reflective sea-ice is substantially reduced leading to enhanced absorption of solar radiation by the high latitude oceans, particularly in summer (sea-ice disappears from the Arctic in summer and is absent from the Antarctic during most of the year). The enhanced ocean heat storage delays the formation of ice in autumn, leading to thinner ice in winter and consequently earlier melting of ice in spring. In the Arctic, the delay in the formation of sea-ice and the consequent reduction in the insulation of the atmosphere from the relatively warm mixed layer surface leads to a maximum warming in autumn. In

winter, there is still a substantial increase in surface air temperature, as the atmosphere is inherently stable and the warming is confined to the lowest model layer as found by Manabe and Wetherald (1975). In summer however, the warming is a minimum, despite increases of up 50 Wm^{-2} in solar heating, because the large thermal inertia of the mixed layer prevents temperatures rising much above 271 K, the melting point of sea-ice. Around Antarctica, the seasonal variation in the temperature change is smaller, probably because the seasonal variation in the control integration is smaller than in the Arctic. The mean warming is also smaller, perhaps because the sea-ice in the control integration is thinner and less extensive than in the northern hemisphere (and than the observed).

Temperature changes over the northern hemisphere continents are generally similar to those over neighbouring oceans. In April, there is a secondary maximum warming near 60°N associated with the earlier removal of highly reflective snow cover in the 4 x CO_2 integration. Over Antarctica, the temperature/albedo feedback is much weaker, as throughout the year in the control integration the surface temperatures are substantially lower than the threshold above which albedo varies. This is largely a result of the height of the Antarctic plateau.

Many of the azonal features in the geographical distribution of surface air temperature changes can be explained in terms of the mechanisms outlined above. Thus for example, during December, January and February (DJF) the surface warming is greatest along the eastern

coasts of northern continents where sea-ice is most extensive and hence sea-ice feedbacks are strongest (Figure 8a). In June, July and August (JJA), there are large changes in surface temperature over the northern hemisphere continents (for example, the south east of North America, and northern Asia near 60°E and 150°E) which are associated with a reduction in soil moisture (see Manabe et al 1981). In areas where evaporation is restricted by soil moisture in the control simulation, a reduction in soil moisture will lower the rate of evaporation, contributing to the increase in surface temperature, so that the fall in the transfer of latent heat from the surface is balanced by the enhanced transfer of sensible heat and longwave radiative cooling. (This is in direct contrast to the changes over a moist surface, where evaporation increases at the expense of sensible heat, as noted earlier). Manabe and Stouffer point out that the temperature changes in Figure 8 are averaged over 3 years only, and that the small scale variations may not be statistically significant.

The global surface warming (4.1 K) is smaller than the 6 K obtained by Wetherald and Manabe (1981) on quadrupling CO_2 in an idealised model with annually averaged insolation. Wetherald and Manabe argue that this is largely because the temperature/albedo feedback in the model with seasonally varying insolation, particularly in the northern hemisphere, is ineffective in summer because of the lack of snow and ice in the control integration, whereas in a model with annual mean insolation, the temperature/albedo

feedback operates all the time. The increase in precipitation and evaporation (6.7%) is also smaller than that found by Wetherald and Manabe (10%) presumably because the temperature change is smaller.

The increase in evaporation varies little with latitude, whereas the main increase in precipitation is in middle- to high-latitudes, as found by Manabe and Wetherald (1975). However, the changes in the hydrological cycle, particularly at the surface, vary with season. For example, there is an enhancement of soil moisture in middle and high northern latitudes in northern winter (Figure 9) where in general the increases in precipitation exceed the increase in evaporation, but there is a reduction in soil moisture, particularly in mid-latitudes, in summer. These changes were investigated in detail by Manabe et al (1981). In the warmer climate, the spring snow melt occurs earlier, so the drying of the land surface which occurs during spring and summer in the control integration commences earlier. The drying is enhanced by stronger evaporation as a result of the additional absorption of solar radiation in late spring due to the reduction in highly reflective snow cover. In middle latitudes, the surface drying is enhanced by a reduction in summer precipitation. Manabe et al note that this is due to the spring to summer reduction in rainfall rate occurring earlier than in the control simulation.

It should be noted that Manabe and Stouffer used a low resolution (15 spectral waves) model which is inadequate to represent the weak baroclinic disturbances which are characteristic of the northern hemisphere mid-latitude summer circulation, and which on the western

side of continents are associated with much of the summer precipitation. Furthermore, the neglect of the oceanic circulation leads to errors in the distribution of sea surface temperatures and sea-ice, which may distort the response of the model to enhanced CO_2. The errors in the sea-ice distribution in Manabe and Stouffer's control integration have already been noted. Even where atmospheric models have been coupled to a dynamical model of the ocean (Manabe et al 1979, Washington et al 1980, Gates et al 1984) there are substantial errors in the simulated sea surface temperatures and sea ice extents. Hence, some studies carried out in the Meteorological Office have followed a different strategy. In the control integration, sea surface temperatures are prescribed from climatology. Since the changes due to CO_2 are sufficiently small to be regarded as a perturbation, the changes in sea surface temperature are prescribed on the basis of a succession of perturbation experiments which approximate equilibrium with increasing accuracy. The advantages of this approach are that the simulated control climate is not distorted by errors in sea surface temperatures and sea-ice, and the simulations attain equilibrium after about one year as opposed to ten or more years needed with a 'slab' ocean. In the Meteorological Office, the consequent saving in computer time has allowed the use of high resolution atmospheric models which are capable of representing baroclinic disturbances throughout the year. The disadvantage of the method is that the prescribed changes (particularly of sea-ice extent) are only approximately in equilibrium, and hence may influence other aspects of the model's response.

In the first Meteorological Office study (Mitchell, 1983a) the response of the ocean was ignored. In the second (Mitchell, 1983a) the ocean temperature increase was assumed to be the same everywhere. In the third (Mitchell and Lupton, 1984), the ocean temperature changes were prescribed as a function of latitude on the basis of the previous two experiments, assuming that the sea surface temperatures respond locally and linearly to changes in the surface heat balance. The changes in sea surface temperature in the tropics and sub-tropics were similar to those found by Manabe and Stouffer (1980), but in high latitudes the method proved unreliable and so changes were based on the GFDL experiments. Analysis of the experiments has concentrated on the changes in the hydrological cycle since the temperature change over most of the earth's surface is prescribed.

The warming of the atmosphere is accompanied by an increase in atmospheric moisture, which in the absence of marked changes in circulation lead to increased precipitation (or more accurately, precipitation minus evaporation) in the main regions of low level atmospheric convergence. Thus, the flux of moisture into high latitudes in winter (Figure 10) is enhanced leading to increased precipitation (Figure 11), soil moisture (Figure 12) and runoff (not shown). The equatorward moisture flux associated with the lower branch of the main Hadley cell is also enhanced, giving enhanced moisture divergence in the winter sub-tropics where there is a tendency to reduced precipitation. These changes are reflected in the geographical distribution of precipitation, which increases in the main regions of atmospheric convergence including the mid-latitude

depression tracks, especially in winter, and along the inter-tropical convergence zone and its extension into the continents. Thus precipitation increases over the southern United States, the Sahel and south east Asia in JJA, Figure 11a, and in eastern South America, South Africa and eastern Australia in DJF, Figure 11b. Precipitation tends to decrease in the regions of enhanced divergence in the sub-tropics. The pattern of the changes in precipitation is broadly similar to that in the earlier experiment with a uniform increase in sea surface temperatures (Mitchell, 1983a) suggesting that changes in precipitation are not critically dependent on the detailed structure of changes in sea surface temperature.

The changes in soil moisture (Figure 12) are remarkably similar to those found in the GFDL experiment using a slab ocean (Figure 9) particularly in the northern hemisphere where in the 4 x CO_2 simulations, middle and high latitudes are wetter in the winter, the sub tropics are drier in winter and mid-latitudes are drier in summer. There are differences as, for example, near 65°N in summer where the drying simulated in the GFDL experiment (Figure 9) is much more pronounced. This may reflect the differences in the control integration. In the GFDL experiment, the high latitude precipitation belt over Eurasia is displaced to the north of its observed position in summer so that there is a pronounced seasonal drying at the surface in the control integration, whereas in the Meteorological Office model, precipitation in the control integration is generally heavier than observed (Mitchell 1983b) and the soil moisture in high latitudes remains close to its maximum allowed value throughout the year. Thus

the earlier onset of the summer drying period in the GFDL experiment has a pronounced effect, whereas in the Meteorological Office model it will have little effect.

Most studies to date have concentrated on the mean changes in climate. The changes in variability may be of greater economic and social importance. Wilson and Mitchell (1986) analysed changes in variability over western Europe in the Meteorological Office experiment. For example, the general reduction in precipitation over southern Europe during JJA is the result of both fewer precipitation events, and reduced precipitation per event.

There is a compromise which can be made between using a "mixed layer" ocean with its attendant errors in the control simulation, and prescribing the distribution of sea surface temperatures and sea-ice with the attendant problem of determining the magnitude of the changes in sea surface temperatures and sea-ice due to enhanced CO_2. The evolution of temperature T to a depth h in the upper ocean (assumed to be well mixed) at each point is given by

$$\rho h C_p \frac{dT}{dt} = S + C \qquad (2)$$

where ρ, C_p are respectively the density and heat capacity of sea water and S is the heat flux through the surface and C is the heat convergence due to oceanic processes (advection, convection etc). An effective C for the model can be determined from an atmospheric simulation with the seasonal variation of sea surface temperatures prescribed from climatology, since $\frac{dT}{dt}$ is known and S can be

diagnosed as the model is integrated. The resulting C can then be specified as a function of time and space in a coupled simulation where S and hence the evolution of temperature $\frac{dT}{dt}$ are determined as the integration proceeds. Thus, the effects of the convergence of heat in high latitudes and the divergence in the equatorial upwelling regions are represented implicitly in the mixed layer model, leading to a much improved simulation of sea surface temperatures and sea-ice extents. Note however, that such a model cannot be used to determine changes in C due to enhanced CO_2. Hansen et al (1984) pioneered the above approach in a low (8° x 10°) resolution model, and some results from a later study using a 5° x 7.5° model (Mitchell et al, 1986a) are presented in the following section.

3.4 Detailed studies with simulated cloud

The earlier GFDL and Meteorological Office experiments used prescribed zonally averaged cloudiness. The parametrization of cloud in climate models is extremely crude, being based on grid box relative humidity, or in the case of convective cloud, the occurrence of moist convection. Nevertheless, several studies have included model-generated cloud cover (for example, Hansen et al, 1984; Washington and Meehl, 1984). The role of changes in cloudiness in CO_2 experiments has been reviewed by Wetherald and Manabe (1986), and results from a recent Meteorological Office experiment using a low resolution atmospheric model coupled to a mixed layer ocean (Figure 13) are fairly typical. Cloud amounts increase at upper levels near the model tropopause, due to deeper convection and

vertical motion, and decrease in the upper and middle troposphere, particularly in the equatorial mid-latitude convection zones. In effect, the height of the model tropopause is increased. In addition, Wetherald and Manabe (1986) note an increase in low stratus cloud in regions where the atmosphere is inherently stable, as over the winter continents and in the marine boundary layer under the sub-tropical anticyclones. This they attribute to enhanced evaporation which increases the flux of moisture into the boundary layer where it is trapped under the climatological inversion.

The changes in cloudiness produce a substantial increase in the sensitivity of climate to thermal forcing (Hansen et al, 1984). The reduction in total cloud noted in most experiments will warm the surface and troposphere, as noted in Section 2. Where high cloud is increased at the expense of more highly reflective low cloud, the loss of solar radiation to space is reduced, and because the effective cloud height is also increased, the emission of longwave radiation to space is also reduced. Hence the warming of the troposphere and surface is further augmented by enhanced solar heating and reduced longwave cooling.

The effect of the cloud feedback is such that the global mean temperature changes due to doubling CO_2 is as large as that due to quadrupling CO_2 in a model with fixed cloud (Manabe and Wetherald, 1986). The patterns of temperature change in the GFDL 4 x CO_2 fixed and 2 x CO_2 variable cloud experiments are remarkably similar (Figure 14, compare Figure 8) except in the Antarctic periphery, particularly

in JJA, where the warming in the 4 x CO_2 experiment is smaller, perhaps owing to the underestimation of Antarctic sea-ice extents in the earlier control integration.

A similar though less marked correspondence exists between the changes in precipitation in the Meteorological Office 4 x CO_2 experiment with prescribed cloud (Figure 11) and the 2 x CO_2 experiment with variable cloud (Figure 15). In both experiments, precipitation increases along the depression tracks and in the summer monsoon regions, and changes little or tends to decrease in the sub-tropics. In general there is a greater tendency for precipitation to increase over the oceans in the 2 x CO_2 experiment; since there were considerable differences in the atmospheric models used in the two experiments, this discrepancy is not necessarily due to the differences in the prescription of cloud or sea surface temperature. The problem of model dependence of results is discussed in more detail by Mitchell et al (1986a). Note the tendency in the 2 x CO_2 experiment for the inter-tropical convergence zone to shift polewards in the summer hemisphere. (In general, the distribution of changes in precipitation in simulations with increased CO_2 agree less well than the distribution of changes in temperature (Schlesinger and Mitchell, 1986). This is largely due to the greater temporal and spatial variability of precipitation and to the large variation in precipitation patterns in control simulations from different models).

In general, changes in soil moisture are more stable, particularly outside the tropics. As noted earlier, there is a general tendency in the GFDL and Meteorological Office experiments for the land surface in northern middle and high latitudes to become drier during summer in the enhanced CO_2 simulations. This is particularly true in studies with model generated cloud (Figure 16). One may speculate that the reduction in evaporation associated with the drier surface may reduce boundary layer cloud, producing a further drying of the surface and so forth.

3.5 Analysis of feedback in 3-dimensional models

Given the marked increase in the sensitivity of simulated climate due to the introduction of cloud feedback, it is instructive to consider the relative strength of the various feedbacks deduced from the 3-dimensional models (Hansen et al, 1984; Dickinson, 1985). It has been the practice to analyse feedbacks using a simple globally averaged energy balance model (although it is not obvious that this is appropriate for highly localised feedbacks such as those due to sea-ice). ΔT, the departure of globally averaged temperature from equilibrium, is given by

$$C \frac{d\Delta T}{dt} + \lambda \Delta T = \Delta Q \qquad (3)$$

where C is the heat capacity of the system, t is time, ΔQ is the external perturbation and λ is the feedback parameter. At equilibrium, $\Delta T = \Delta Q/\lambda$; the smaller λ, the weaker the restoring term on the left hand side of the equation, and the greater the sensitivity

of the model. In the absence of internal feedbacks, $\lambda = 3.7\ Wm^{-2}\ K^{-1}$, assuming the unperturbed earth atmosphere system behaves like a black body with an effective emitting temperature of 255 K and has a shortwave reflectivity of 30%.

Estimates of the contribution to λ due to water vapour feedback are typically $-1.5\ Wm^{-2}K^{-1}$ (Mitchell, 1983a; Hansen et al, 1984); whereas sea-ice contributes about $-0.4\ Wm^{-2}K^{-1}$ (Hansen et al 1984) and cloud about $-0.9\ Wm^{-2}K^{-1}$ (Mitchell et al, 1986a, Hansen et al 1984). If we assume that ΔQ due to doubling CO_2 is about $4\ Wm^{-2}$ (for example Lal and Ramanathan, 1984), then the first two feedbacks increase the equilibrium change due to doubling CO_2 from 1.1 K to 2.2 K (Table 3). Although the strength of the cloud feedback is only about half of that due to the water vapour and sea-ice feedbacks combined, cloud feedback produces a further doubling of the model's sensitivity. This is because λ has already been reduced by the other two feedbacks and the sensitivity is inversely proportional to λ.

The general circulation models used to date have assumed that cloud optical properties are invariant with climate. As noted in section 2, there has been speculation that the general increase in atmospheric specific humidity would lead to an increase in cloud liquid water content and hence the reflectivity of cloud, providing a negative climate feedback. The results of Somerville and Remer (1984) imply that the resulting negative feedback is sufficient to counteract all the positive feedbacks in Table 3. It must be pointed out that

Somerville and Remer make some sweeping assumptions in their parametrization. The magnitude of cloud optical effects is extremely uncertain, and is a priority for future research.

3.6 Oceanic effects

The use of three-dimensional coupled ocean-atmosphere models to study the effects of CO_2 has largely been limited to low resolution simulations using annually averaged insolation and idealised geography (Spelman and Manabe, 1984; Manabe and Bryan, 1985). Manabe and Bryan performed 6 experiments with CO_2 concentrations ranging from 150 to 2400 ppm. Equilibrium was reached using the acceleration techniques described by Bryan (1984). The zonal mean temperature changes in the upper ocean due to a four-fold increase in CO_2 (Figure 17, from Spelman and Manabe, 1984) follow those in the atmosphere, with smallest changes in low latitudes, due to the effects of moist convection, and the greatest warming in high latitudes, due to sea-ice albedo feedback and the weakening of the surface inversion). The large surface warming in high latitudes is propagated into the deep ocean where it is advected equatorwards. Manabe and Bryan comment that the intensity of the model's oceanic meridional circulation changes little for CO_2 concentrations above 300 ppm. The coefficient of expansion of sea water increases sharply with temperature. Hence, the greater warming in high latitudes is largely compensated by the larger coefficient of thermal expansion in low latitudes and the meridional density gradient is changed little.

3.7 The transient response

So far, we have considered only the equilibrium response of climate to enhanced atmospheric CO_2 concentrations. The time dependent response of climate to an increase in CO_2 concentrations is likely to be slowed by the large thermal inertia of the oceans. Since the effective thermal inertia of the oceans is dependent on the ocean circulation and varies with latitude, it is possible, as suggested by Schneider and Thompson (1981), that the transient response of the climate to enhanced atmospheric CO_2 could differ substantially from the equilibrium response. Spelman and Manabe (1984) investigated the effect of 'switching on' a four-fold increase in CO_2 using synchronous coupling between the ocean and atmosphere (that is, the devices to accelerate convergence to equilibrium were removed) and compared the response with that at equilibrium. After 25 years, the fractional response in the upper atmosphere and surface layer of the ocean was generally uniform with latitude (Figure 18, lower panel). The greatest penetration of the warming in the deep ocean occurred near 55°. At higher latitudes, the warming is largely confined to the surface layer, due to the presence of a stable layer of fresher less dense water which was the result of the excess of precipitation over evaporation. The oceanic response is discussed in more detail by Bryan and Spelman (1985). Spelman and Manabe suggest that provided the time constant for increasing CO_2 concentrations is greater than 25 years, the transient response of zonally averaged temperature should resemble equilibrium response. The ocean model used in their experiments is highly idealised, does not resolve mesoscale eddies and

substantially underestimates the strength of the meridional circulation. As Spelman and Manabe point out, the transient behaviour of their model needs to be verified against observational data, and their experiment repeated with a more realistic model before we can have confidence in these results.

4. Detection

Given an estimated increase of 25 to 30% in the concentration of atmospheric CO_2 since 1860, it is pertinent to ask whether or not the effect of such an increase can be detected in the observational record. The answer to this question is obscured by several uncertainties.

1. The pre-industrial concentration of CO_2 is variously reported to have been in the range 260 to 280 ppm (WMO, 1983).

2. Estimates of the equilibrium response to CO_2 vary by a factor of 3 (US National Research Council, 1983), owing mainly to the uncertainties in feedbacks through changes in cloud and sea-ice discussed above. However, these uncertainties also affect the transient response as the response time of the idealized system described by equation (3) is $C/\lambda = C\ \Delta T_e/\Delta Q$ where ΔT_e is the equilibrium temperature change. Thus, the larger the equilibrium response, the smaller the fractional response in a given time, so that the absolute response on a short time scale is only weakly dependent on the magnitude of the equilibrium response.

3. It is uncertain to what degree the uptake of heat by the oceans will slow the approach of climate to equilibrium, because of our lack of detailed knowledge of vertical mixing processes in the ocean.

4. There are considerable variations in the observed global mean surface temperature record (Figure 19, from Folland et al, 1984) which are obviously not a result of increased CO_2. Indeed, some of the observed oscillations may be due to random oscillation in the ocean-atmosphere system (Hasselmann, 1979). The problem of determining the present increase in global mean temperature due to increased CO_2 has been considered by Hansen et al (1981), Wigley and Schlesinger (1985) and others using extremely simple 1- or 2-dimensional models. For example, on the basis of Wigley and Schlesinger's assumptions, the estimated warming from 1880 to date due to increased CO_2 ranges from 0.3 K (1880 CO_2 concentration of 280 ppmv, 1.5 K equilibrium temperature increase due to doubling CO_2, large vertical mixing coefficient) to 1 K (260 ppmv initial CO_2 concentration, 4.5 K equilibrium increase at doubling, small vertical mixing coefficient). The larger value appears to be inconsistent with the observational record. Madden and Ramanathan (1980), Wigley and Jones (1981) and Parker (1985a, b) have considered strategies for detecting the effect of increased CO_2.

5. Concluding remarks

Following Manabe (1983), the physical responses of climate to enhanced CO_2 concentrations determined from recent numerical studies are listed below.

1. There is a warming of the troposphere and a cooling of the stratosphere because the enhancement of atmospheric CO_2 concentrations increases the opacity of the atmosphere to longwave radiation, and raises the effective emitting level of the atmosphere.

2. The annual mean surface warming is largest in high latitudes because of sea-ice and snow albedo feedbacks, the inherent low level stability in high latitudes, and perhaps the enhanced advection of latent heat from lower latitudes.

3. Over the Arctic Ocean and surrounding regions, the warming has a large seasonal dependence, and is a minimum in summer. There is little seasonal dependence in temperature changes in low latitudes.

4. Global mean rates of evaporation and precipitation increase. This is due to enhanced radiative heating at the surface in the warmer, moister, CO_2 enriched atmosphere.

5. The snowmelt season begins earlier.

6. Sea-ice is less extensive (and thinner, at least in those studies from which such information is available).

7. Precipitation and (where reported) runoff increase in high latitudes, because of the enhanced poleward transport of moisture in the warmer, moister atmosphere.

8. In most studies to date, soil moisture is reduced over much of the northern middle and high latitude continents in summer. This change is due to one or more of the following factors: earlier snowmelt, enhanced evaporation and reduced precipitation. Soil moisture also decreases in Northern subtropics in winter as a result of enhanced atmospheric moisture divergence.

9. The response to CO_2 is greatly enhanced in simulations with model generated cloud. Both a reduction in total cloud and an increase in mean cloud height appear to contribute to the enhanced surface warming.

10. The uncertainties in past levels of CO_2, the equilibrium sensitivity of climate to CO_2, the transient response of the ocean, and the temporal variability in the instrumental record of temperature during the last century are such that it is not possible to prove whether or not the climatic effects of CO_2 increases in the atmosphere to date have been detected.

Recent work has demonstrated that simplified models, although invaluable for identifying physical mechanisms, can produce misleading results since they may omit processes relevant to climate change, or they may not weight competing mechanisms correctly. In the same way, it must be recognised that the most sophisticated models in use at present contain many simplifications and approximations, which may distort the simulated response to enhanced CO_2. In particular, the horizontal resolution employed in most climate models to date is inadequate to provide an accurate simulation of present day climate, and so such models are unlikely to provide reliable guidance on regional climate change.

In looking to the future, there are three outstanding priorities in understanding and predicting of climate change due to increased CO_2. The first is to reduce the large uncertainties in the equilibrium response of climate to increased CO_2. This will require a more careful evaluation of the feedbacks due to changes in water vapour, sea-ice, cloud cover and cloud optical properties. The last named factor is probably the least well known, potentially giving rise to the greatest uncertainty, and is arguably the subject where further research is most urgently needed. The second priority is the need to determine more accurately the transient response of climate to enhanced CO_2, and in particular, the extent to which the oceans slow the approach to equilibrium. The third priority is to determine the natural variability of the ocean-atmosphere system on a time scale of up to a century, and the contribution of other factors. Once these aims have been achieved, it will be clear what warming should have occurred over the last century due to the effects of increased CO_2, and when changes in climate will become apparent.

Since the oceans are expected to slow the response to increasing CO_2, the actual warming at a given time is likely to be substantially smaller than the equilibrium warming, even if CO_2 concentrations no longer continue to increase, so it may not be prudent to wait until the effects of CO_2 are unequivocally demonstrated. Hence there is also a need to maintain or expand research into other aspects of the effects of increasing CO_2, including changes in climate likely to have economic and social consequences. This will require a more accurate simulation of regional climate and changes in climatic variability, and a more detailed simulation of boundary layer and surface processes.

Many disciplines are involved in assessing the human consequences of increases in atmospheric CO_2. To do so, they require accurate predictions of potential changes in climate. Numerical models of climate provide the most promising means of making those predictions. Since, unlike those involved in numerical weather prediction, we cannot verify the detailed behaviour of our models using case histories, our confidence in the model's performance must depend on the degree to which it is based on physical principles.

References

Augustsson, T and Ramanathan, V 1977 A radiative, convective model study of the CO_2 climate problem. J. Atmos. Sci. 34, 448-51.

Bach, W; Crane, A J; Berger, A L and Longhetto, A 1983 Carbon Dioxide: Current Views and Developments in Energy/Climate Research. D. Reidel Publishing Company. Dordrecht/Boston/Lancaster.

Bolin, B; Degens, E T; Kempe, S Ketner, P 1979 The Global Carbon Cycle, SCOPE 13, John Wiley and Sons, New York.

Bryan, K 1984 Accelerating the convergence to equilibrium of ocean-climate models. J. Phys. Oceanogr. 14 (4) 666-673.

Bryan, K and Spelman, M J 1985 The ocean's response to a CO_2 induced warming. J. Geophys. Res. 90, C6, 11679-11688.

Callendar, G S 1938 The artificial production of carbon dioxide and its influence on temperature. Q.J.R. Met. Soc. 64, 223-240.

Clarke, W C 1982 Carbon Dioxide Review: 1982 (Ed. W C Clark). Clarendon Press, Oxford; Oxford University Press, New York 469 pp.

Dickinson, R E 1985 Modelling of future climate. The WMO/ICSU/UNEP International Assessment of the Impact of an Increased Atmospheric Concentration of Carbon Dioxide on the Environment. (To be published).

Feigelson, E M 1978 Preliminary Radiation Model of a cloudy atmosphere I. Structure of clouds and solar radiation. Beitr. Phys. Atmos. 51, 203-229.

Folland, C K; Parker, D E and Kates, F E 1984 Worldwide Marine Temperature Fluctuations 1856-1981. Nature 210, 670-3.

Gates, W L; Han, Y J and Schlesinger, M E 1985 The Global Climate Simulated by a Coupled Atmosphere-Ocean General Circulation Model, Preliminary Results. In 'Coupled Ocean-Atmosphere Models' (ed. J C J Nihoul). Elsevier Oceanography Series, 40 (Amsterdam, new York, oxford, Tokyo).

Hansen, J E; Johnson, D, Lacis, A; Lebedeff, S; Lee, P; Rind, D and Russell, G 1981 Climate impact of increasing atmospheric carbon dioxide. Science 213 957-966.

Hansen, J; Lacis, A; Rind, D; Russell, G; Stone, P; Fung, I; Ruedy, R and Lerner, J 1984 Climate Sensitivity and Analysis of Feedback Mechanisms. In Climate Sensitivity (ed. J Hansen and T Takahashi) Geophysical Monograph 29, 130-163. American Geophysical Union, Washington DC.

Hasselmann, K 1979 On the problem of multiple time scales in climate modelling. In 'Man's Impact on Climate' (eds. Bach, Pankrath and Kellogg). Developments in Atmospheric Science, 10, 43-55. Elsevier (Amsterdam, Oxford, New York).

Idso, S B 1980 The climatological significance of a doubling of earth's atmospheric carbon dioxide concentration. Science, 207, 1462-1463.

Kiehl, J T and Ramanathan, V 1983 Radiative Heating due to increased CO_2: The role of H_2O continuum absorption in the 12-18 μm region. J. Atmos. Sci. 31, 2923-2926.

Lal, M and Ramanathan, V 1984 The effects of moist convection and water vapour radiative processes on climate sensitivity. J. Atmos. Sci. 41, 2238-2249.

Liss, P S and Crane, A J 1983 Man-made Carbon Dioxide and Climatic Change. A review of scientific problems. Geo Books, Norwich.

Luther, F M and Fouquart, Y 1984 The intercomparison of radiation codes in climate models (ICRCCM). Longwave clear sky calculations. WCP-93, WMO, Geneva.

Madden, R A and Ramanathan, V 1980 Detecting Climate Change due to increasing Atmospheric Carbon Dioxide, Science, 209 763-768.

Manabe, S 1983 Carbon Dioxide and Climatic Change. Advances in Geophysics 25, 39-82 Academic Press Inc.

Manabe, S and Bryan, K, Jr. 1985 CO_2-induced Change in a Coupled Ocean-Atmosphere Model and its Paleoclimatic Implications. J. Geophys. Res. 90, C11, 11, 689-11, 707.

Manabe, S and Wetherald, R T 1980 On the distribution of climate change resulting from an increase in the CO_2 content of the atmosphere. J. Atmos. Sci. 37, 99-118.

Manabe, S and Stouffer, R J 1980 Sensitivity of a global climate model to an increase in the CO_2 concentration in the atmosphere. J. Geophys. Res. 85, 5529-5554.

Manabe, S and Strickler, R F 1964 Thermal equilibrium of the atmosphere with a convective adjustment. J. Atmos. Sci. 21, 361-385.

Manabe, S and Wetherald, R T 1967 Thermal equilibrium of the atmosphere with a given distribution of relative humidity. J. Atmos. Sci. 24, 241-259.

Manabe, S and Wetherald, R T 1975 The effects of doubling the CO_2 concentration on a general circulation model. J. Atmos. Sci. 32, 3-15.

Manabe, S; Bryan, K and Spelman, M J 1979b A global ocean-atmosphere climate model with seasonal variation for future studies of climate sensitivity. Dynamics of Atmospheres and Oceans, 3, 393-426.

Manabe, S; Wetherald, R T and Stouffer, R T 1981 Summer dryness due to an increase of atmospheric CO_2 concentration. Climatic Change 3, 347-385.

Marland, G and Rotty, R M 1983 Carbon dioxide emissions from fossil fuel CO_2 emissions (DOE/NBB-0036). US Dept. of Energy, Washington DC.

Mitchell, J F B 1983a The seasonal response of a general circulation model to changes in CO_2 and sea surface temperature. Q.J.R. Met. Soc., 109, 113-152.

Mitchell, J F B 1983b The hydrological cycle as simulated by an atmospheric general circulation model. In 'Variations in the Global Water Budget' (eds. Street-Perrott, Beran and Ratcliffe) D Reidel Publishing Company, Dordrecht/Boston/ Lancaster.

Mitchell, J F B 1986 Climate Sensitivity and Past Climates: Evidence from numerical studies. DCTN 36, Meteorological Office, Bracknell, Berkshire RG12 2SZ.
Submitted to Proceedings of NATO/NSF Workshop 'Abrupt Climatic Changes', Grenoble, 16-22 October 1985.

Mitchell, J F B and Lupton, G 1984 A 4 x CO_2 experiment with prescribed changes in sea temperatures. Progress in Biometeorology, 3, 353-374.

Mitchell, J F B, Wilson, C A and Cunnington, W M 1986a On CO_2 climate sensitivity and model dependence of results. Submitted for publication. (Available as DCTN 28, Dynamical Climatology Branch, Meteorological Office, Bracknell, Berkshire RG12 2SZ, England).

Mitchell, J F B; Wilson, C A; Ingram, W J and Cunnington, W M 1986b Numerical studies of the effect of increased atmospheric carbon dioxide on climate. (Final report of CEC Contract CL-114-UK(H)), available from Meteorological Office, Bracknell, Berkshire RG12 2SZ, England.

Newell, R E and Dopplick, T G 1979 Questions concerning the possible influence of anthropogenic CO_2 on atmospheric temperature. J. Appl. Meteor. 18, 822-825.

Oeschger, H and Stauffer, B 1986 Review of the history of atmospheric CO_2 recorded in ice cores. In 'The changing carbon cycle: a global analysis' (ed. J R Trabalka and D E Reichle) Springer-Verlag, New York.

Ohring, G and Clapp, P F 1980 The effect of changes in cloud amount on the net radiation at the top of the atmosphere. J. Atmos. Sci. 37, 447-454.

Parker, D E 1985a On the detection of temperature changes induced by increasing atmospheric carbon dioxide. Q.J.R. Met. Soc. 111, 587-601.

Parker, D E 1985b A strategy for early detection of climate change. Report of the sixth session of the Joint Scientific Committee. WMO/TD No. 54 Appendix B. WMO, Geneva.

Ramanathan, V 1981 The role of ocean atmosphere interactions in the CO_2 climate problems. J. Atmos. Sci. 38, 918-930.

Roach, W T and Slingo, A 1979 A high resolution infrared radiative transfer scheme to study the interaction of radiation with cloud. Q.J.R. Meteorol. Soc. 105, 603-614.

Rowntree, P R and Walker, J 1978 The effects of doubling the CO_2 concentration on radiative-convective equilibrium. In Carbon Dioxide, Climate and Society, J Williams (ed.) 181-191, Pergamon Press, Oxford.

Schlesinger, M E and Mitchell, J F B 1985 Model Projections of Equilibrium Climatic Response to Increased CO_2 concentration. In 'Projecting the Climatic Effects of Increasing Carbon Dioxide'. (ed. M C MacCracken and F M Luther) US Dept. of Energy, Washington DC.

Schneider, S H and Thompson, S L 1981 Atmospheric CO_2 and Climate: Importance of the transient response. J. Geophys. Res. 86, (C4) 3135-3147.

Somerville, R C J and Remer, L A 1984 Cloud Optical Thickness Feedbacks in the CO_2 Climate Problem. J. Geophys. Res. 89, 9668-9672.

Spelman, M J and Manabe, S 1984 Influence of Oceanic Heat Transport Upon the Sensitivity of a Model Climate. J. Geophys. Res. 89, 571-586.

Stephens, G L 1978 Radiation profiles in extended water clouds II: Parametrisation Schemes. J. Atmos. Sci. 35 2123-2132.

Stone, H M and Manabe, S 1968 Comparison among various numerical models designed for computing infrared cooling. Mon. Wea. Rev. 96, 735-741.

Trabalka, J R 1985 Atmospheric Carbon Dioxide (ed. J R Trabalka) DOE/ER-239, US Dept. of Energy. Washington DC.

US Dept. of Energy 1985a Atmospheric Carbon Dioxide and the Global Carbon Cycle (ed. J R Trabalka). Report DOE/ER-0239, US Dept. of Energy, Washington DC.

US Dept. of Energy 1985b Projecting the Climatic Effects of Increasing Carbon Dioxide (eds. M C MacCracken and F M Luther) US Dept. of Energy, Washington DC.

US Dept. of Energy 1985c Detecting the Climatic Effects of Increasing Carbon Dioxide (eds. M C MacCracken and F M Luther) Report No. DOE/ER-0235. US Dept. of Energy, Washington DC.

US Dept. of Energy 1985d Direct effects of increasing carbon dioxide on vegetation (eds. B R Strain and J D Cure) Report No. DOE/ER-0238. US Dept. of Energy, Washington DC.

US National Research Council 1983 Changing climate (report of the Carbon Dioxide Assessment Committee) National Research Council. National Academy Press, Washington DC.

US National Research Council 1982 Carbon Dioxide and Climate: A scientific assessment. National Academy Press, Washington DC.

US National Research Council 1979 Carbon Dioxide and Climate: A scientific assessment. National Academy Press. Washington DC.

WMO 1983 Report of the WMO (CAS) Meeting of Experts on the CO_2 concentrations from pre-industrial times to IGY, WCP-55 (WMO, Geneva).

Washington, W M and Meehl, G A 1984 Seasonal Cycle Experiment on the Climate Sensitivity Due to a Doubling of CO_2 with an Atmospheric General Circulation Model coupled to a Simple Mixed Layer Ocean Model.
J. Geophys. Res. 89 9475-9503.

Washington, W M; Semtner, A J; Knight, D J and Mayer, T A 1980 A general circulation experiment with a coupled atmosphere, ocean and sea ice model.
J. Phys. Oceanogr. 10 1887-1908.

Watts, R G 1982 Further discussions of 'Questions concerning the possible influence of enthropogenic CO_2 on atmspheric temperature', J. Appl. Meteor. 21, 243-247.

Wetherald, R T and Manabe, S 1981 Influence of seasonal variation upon the sensitivity of a model climate.
J. Geophy. Res. 86 1194-1204.

Wetherald, R T and Manabe, S 1986 'An investigation of cloud cover change in response to thermal forcing'.
Climate Change (to appear).

Wigley, T M L and Jones, P D 1981 Detecting CO_2-induced climate change.
Nature, 292, 205-208.

Wigley, T M L and Schlesinger, M E 1985 Analytical solution for the effect of increasing CO_2 on global mean temperature.
Nature 315, 649-652.

WMO/ICSU/UNEP 1985 WMO/ICSU/UNEP International Assessment of the Impact of an Increased Atmospheric Concentration of Carbon Dioxide on the Environment. (To be published).

Wilson, C A and Mitchell, J F B 1986 The 5-layer model climate over Western Europe and the frequency of occurrence of extreme values of temperature, precipitation and wind for selected grid boxes: the changes with 4 x CO_2 and prescribed sea surface temperatures. To be submitted for publication.

TABLE 1. Thermal Reponse Times of various components of the climate system.

Component	Approximate Response Time (years)
Troposphere	0.05
Lower Stratosphere	0.2-0.5
Land Surface	0.2-1.0
Upper Ocean	5-10
Deep Ocean	100-1000
Continental Ice Sheets	~ 10,000

TABLE 2. Increase in surface air temperature and precipitation due to doubling CO_2 deduced from GFDL studies. a and b refer to the radiation schemes used by Manabe and Strickler (1964) and Stone and Manabe (1968) respectively. The brackets denote values obtained by halving results from a 4 x CO_2 experiment.

Model	Temperature (K)		Precipitation %
	a	b	
1-D Radiative-Convective	2.4	1.9	
3-D Swamp Ocean	2.9		7
3-D Mixed Layer Ocean:			
Prescribed cloud		(2.0)	3.4
Variable cloud		4.0	8.7

TABLE 3. Typical values of internal feedbacks

Feedback	Contribution to feedback factor ($Wm^{-2}K^{-1}$)	Feedback factor λ (Cumulative, $Wm^{-2}K^{-1}$)	Cumulative change in surface temperature, K ($\Delta Q=4\ Wm^{-2}$)
None		3.7	1.1
Water Vapour	-1.5	2.2	1.7
Sea ice/snow	-0.4	1.8	2.2
Cloud cover	-0.9	0.9	4.4

Figure Captions

Figure 1. Concentration of atmospheric CO_2 at Mauna Loa Observatory, Hawaii, ppm (parts per million of dry air). The horizontal bars represent annual averages. Data were obtained by C D Keeling, and the diagram is reproduced from Trabalka (1985).

Figure 2. Fossil fuel CO_2 emissions: 1860-1982 (Marland and Rotty, 1983, reproduced in Trabalka, 1985).

Figure 3. Effect of increasing CO_2 on the vertical profile of temperature (schematic).

Figure 4. Spectral distribution of longwave radiation at the surface under a mid-latitude profile of temperature and gaseous absorbers (schematic, adapted from Roach and Slingo, 1979).

Figure 5. Effect of doubling CO_2 in a radiative convective model with equinoctial insolation appropriate to 35°N, assuming average cloud and fixed relative humidity. Dashed line, constant lapse rate; solid line, saturated adiabatic. (P R Rowntree, personal communication).

Figure 6. Height-latitude diagram of zonally averaged temperature changes (K) due to doubling CO_2 in an idealized climate model (Manabe and Wetherald, 1975).

Figure 7. Time-latitude diagram of changes in zonally averaged surface air temperature (K) due to quadrupling CO_2 in a low resolution climate model with prescribed cloud (Manabe and Stouffer, 1980).

Figure 8. Changes in surface air temperature (K) due to quadrupling CO_2 in a low resolution climate model with prescribed cloud (Manabe and Stouffer, 1980).

(a) June to August. (b) December to February.

Figure 9. Time-latitude diagram of changes in zonally averaged soil moisture (cm) due to quadrupling CO_2 in a low resolution climate model with prescribed cloud (Manabe and Stouffer, 1980).

Figure 10. Northward fluxes of moisture (10^{13} kg/day) in a 4 x CO_2 study with climatological cloud and prescribed changes in sea surface temperatures (Mitchell and Lupton, 1984). Solid line, control integration; dashed line, 4 x CO_2 integration; chain dotted line, 4 x CO_2-control.June to August above, December to February below.

Figure 11. Changes in precipitation in 4 x CO_2 experiment with climatological cloud and prescribed changes in sea surface temperature (Mitchell and Lupton, 1984). Contours at 0, $\pm$1, $\pm$2 mm/day, areas of decrease are stippled. (a) June to August, (b) December to February.

Figure 12. Time latitude diagram of changes in soil moisture (mm) in a 4 x CO_2 experiment with climatological cloud and prescribed changes in sea surface temperature (Mitchell and Lupton, 1984).

Figure 13. Height-latitude diagram of the annually and zonally averaged changes in cloud due to doubling CO_2 in a low resolution climate model (Mitchell et al, 1986b).

Figure 14. Changes in surface temperature due to doubling CO_2 (Manabe and Wetherald, reproduced from Schlesinger and Mitchell (1985)) (a) June to August (b) December to February).

Figure 15. Changes in precipitation due to doubling CO_2 (Mitchell et al, 1986a). Contours at 0, $\pm$ 1, $\pm$2 mm/day, stippled in areas of decrease (a) June to August (b) December to February.

Figure 16. Changes in soil moisture during June to August due to doubling CO_2 in a low resolution climate model (Mitchell et al, 1986b). Solid contours at 0, $\pm$ 2 cm, dashed contours at $\pm$ 1 cm, $\pm$ 5 cm, areas of decrease are shaded.

Figure 17. Height-latitude diagram of zonally averaged equilibrium changes in temperature due to quadrupling CO_2 in an idealized coupled ocean-atmosphere model (Spelman and Manabe, 1984).

Figure 18. Height-latitude diagram of zonally averaged changes in temperature 25 years after quadrupling CO_2 amounts in an idealized coupled ocean model (upper panel) and percentage of equilibrium response (lower panel). From Spelman and Manabe, 1984.

Figure 19. Corrected anomalies (relative to 1951-60) of (a) global sea surface temperature and (b) global night-time marine air temperature (adapted from Folland et al, 1984).

Figure 1

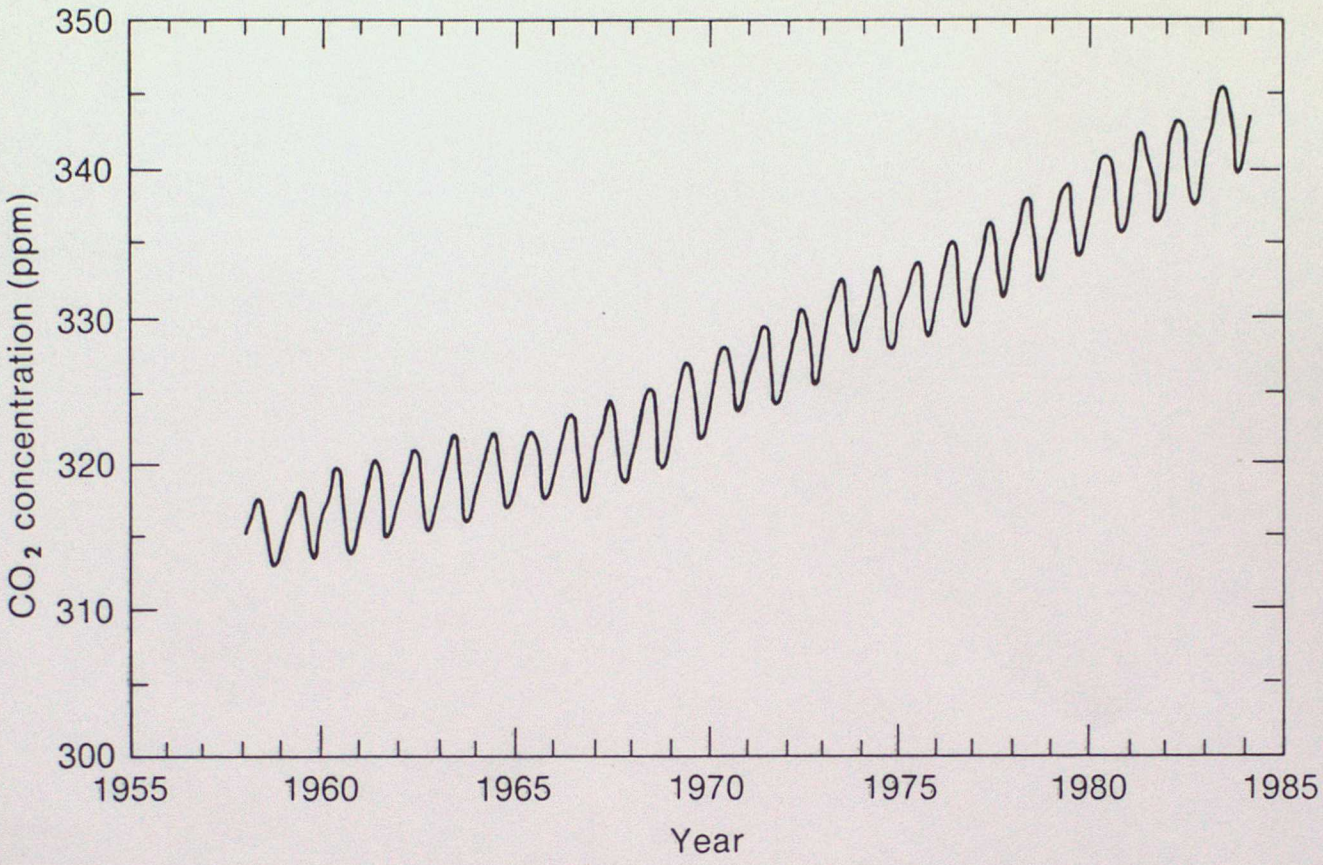

Figure 2

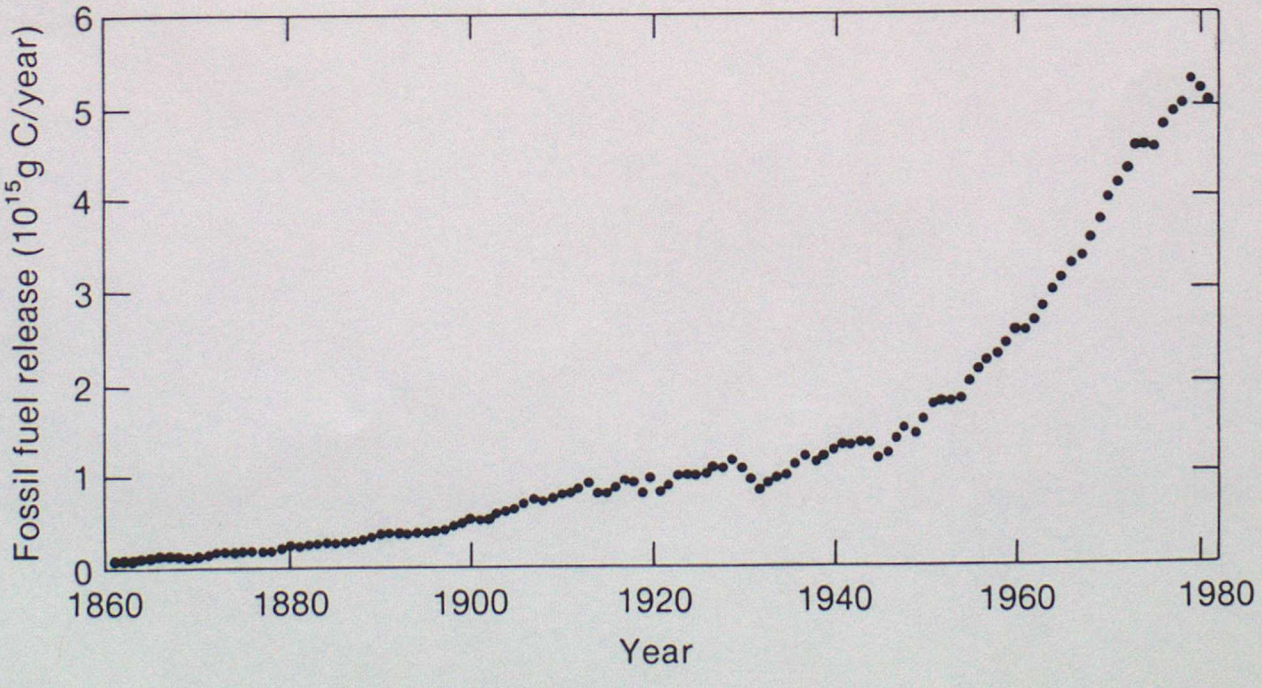

Figure 3

Effect of increasing CO_2 on the vertical profile of temperature (schematic)

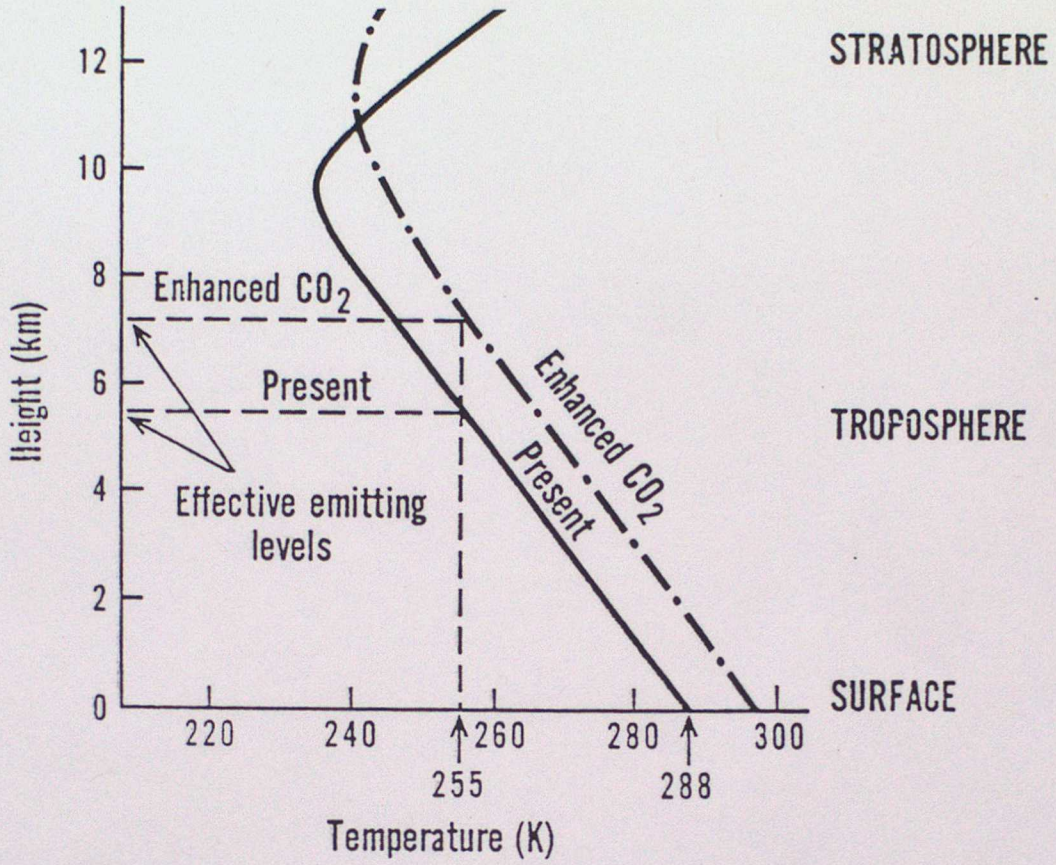

Figure 4

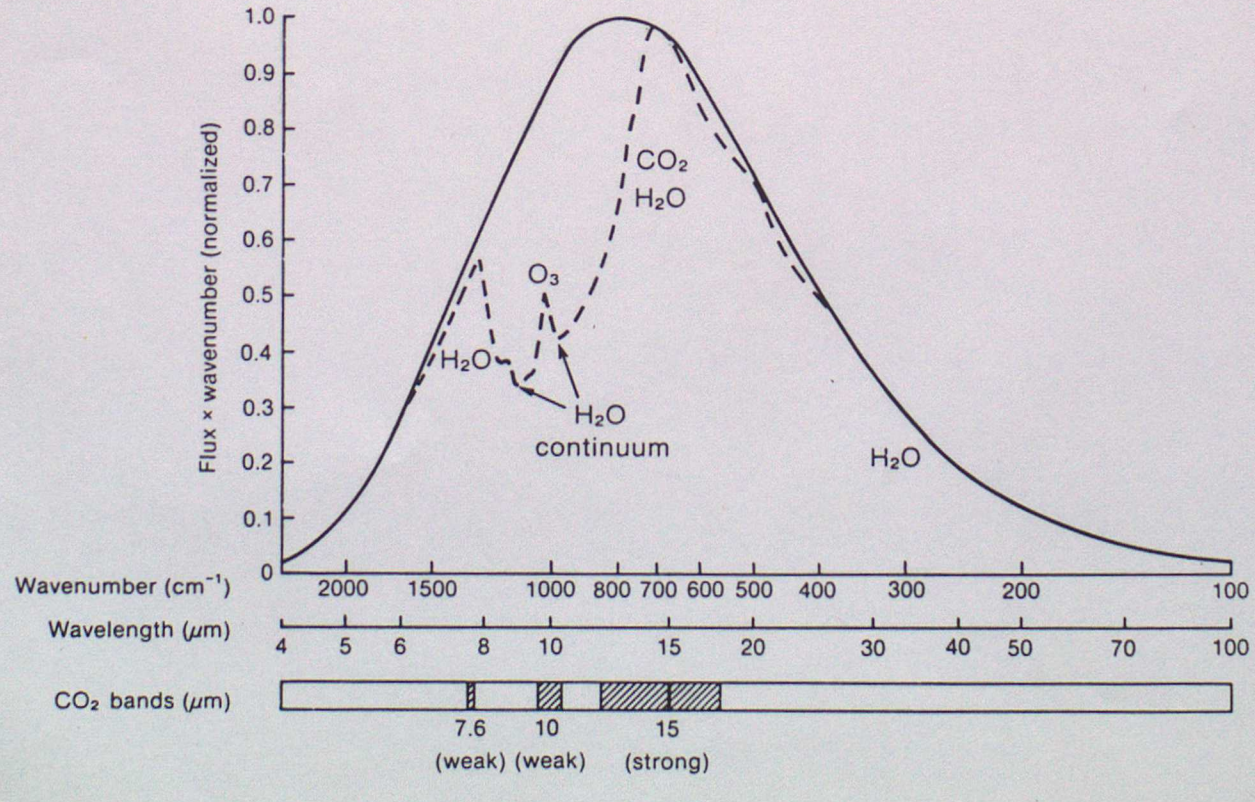

Figure 5

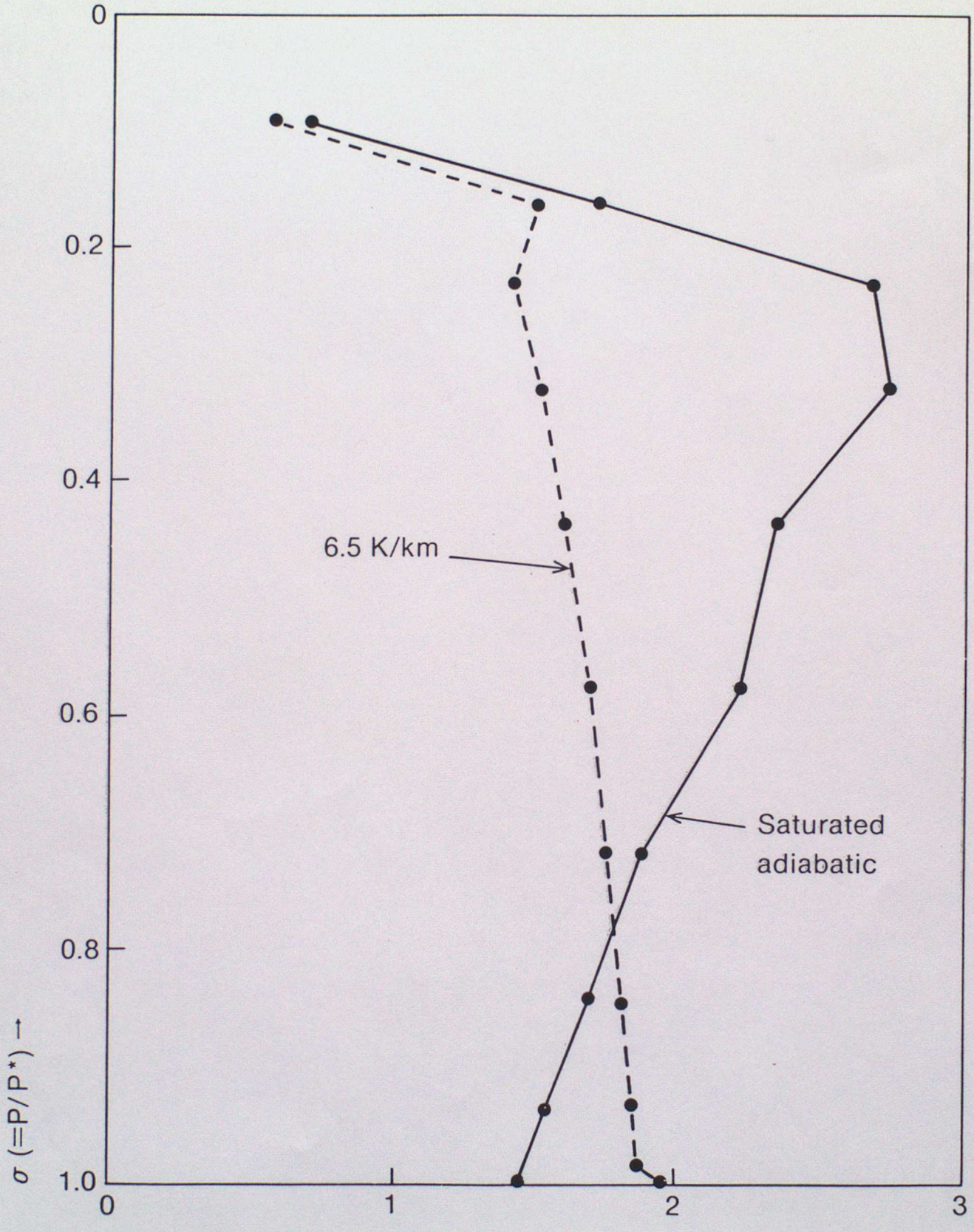

CO_2 doubling effect in single column model
(equinox; 35 °N; average cloud; fixed relative humidity)

Figure 6

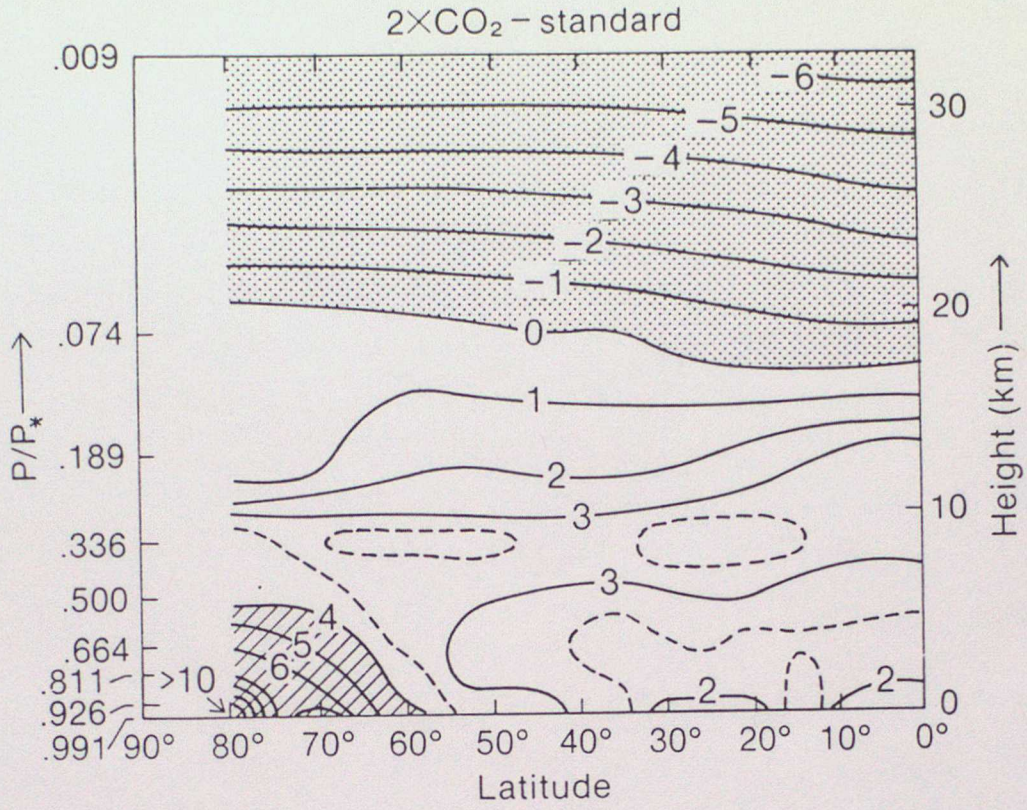

Figure 7

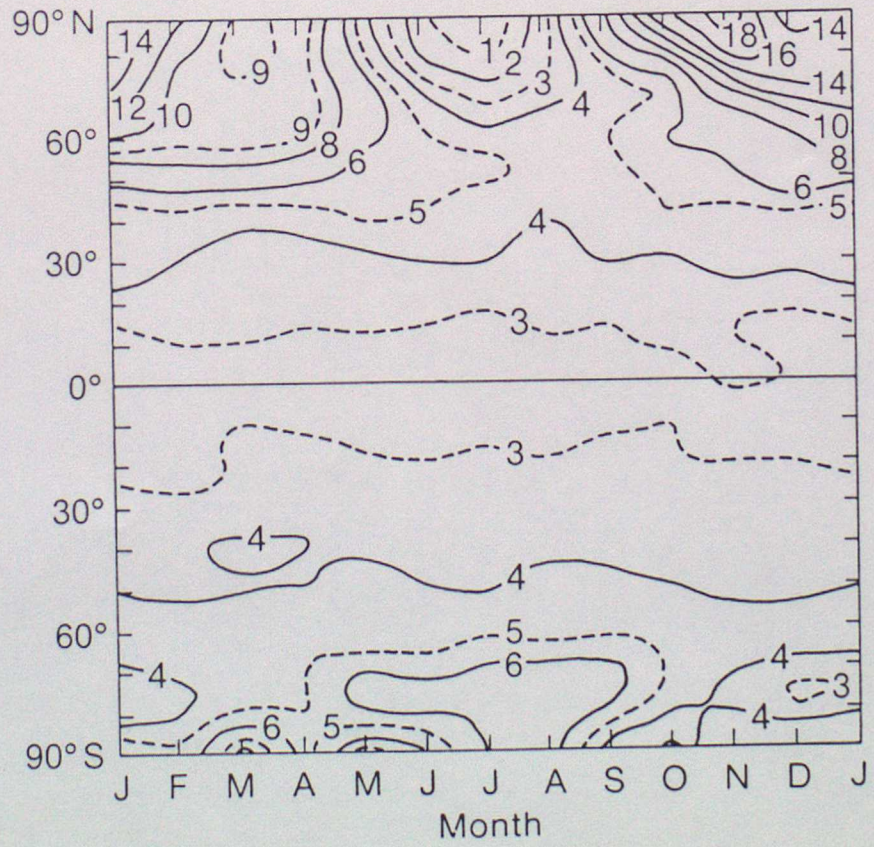

Figure 8a

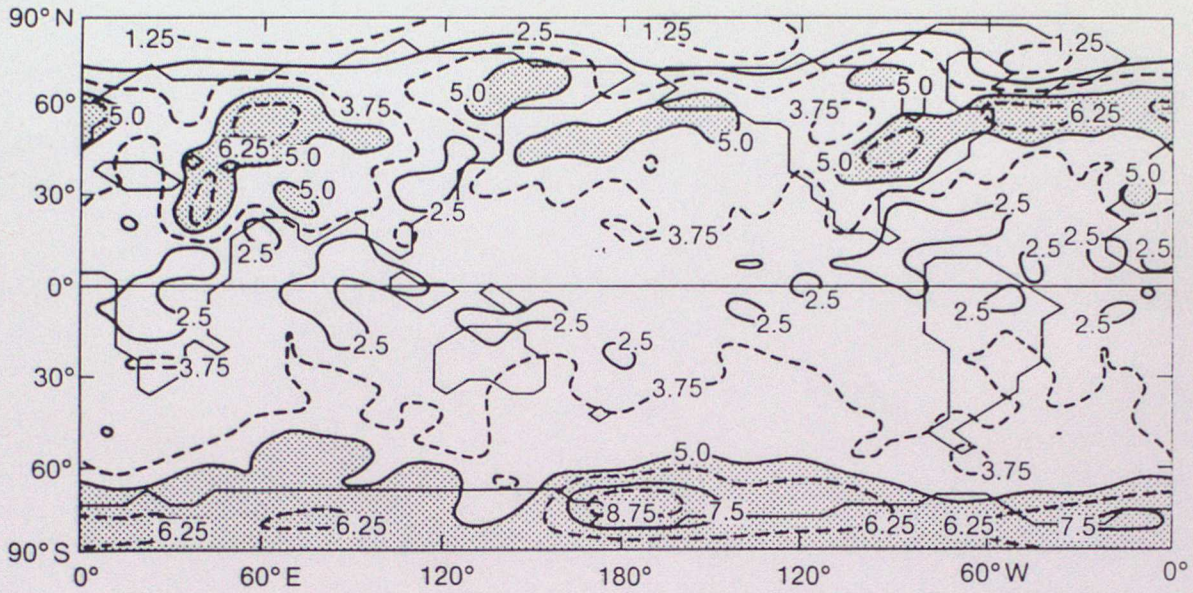

Figure 8b

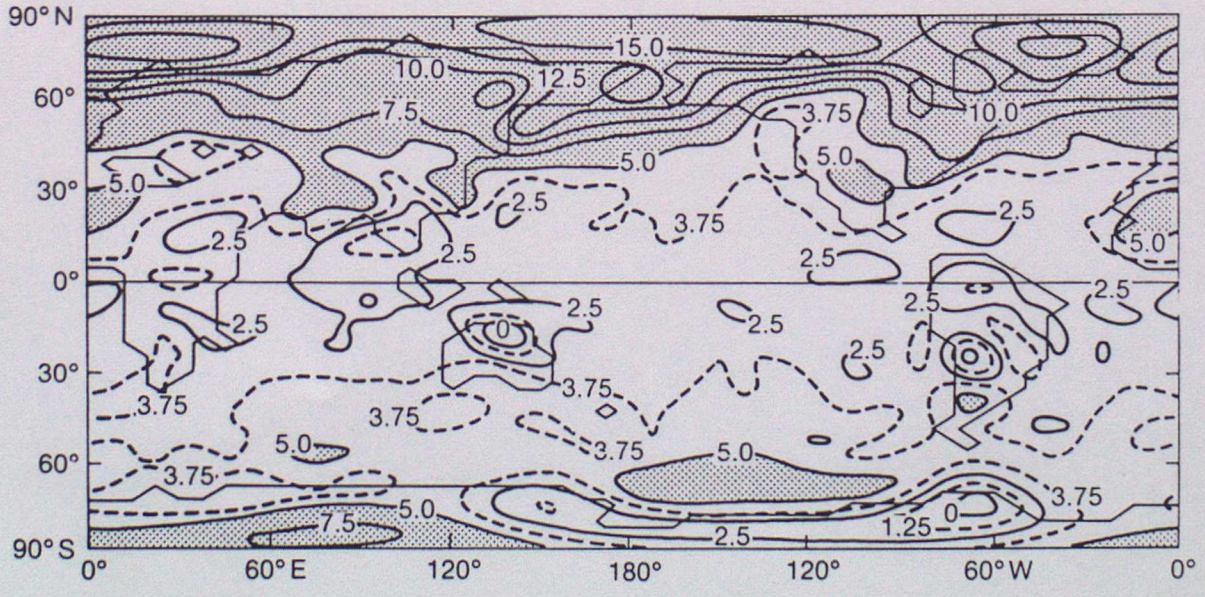

Figure 9

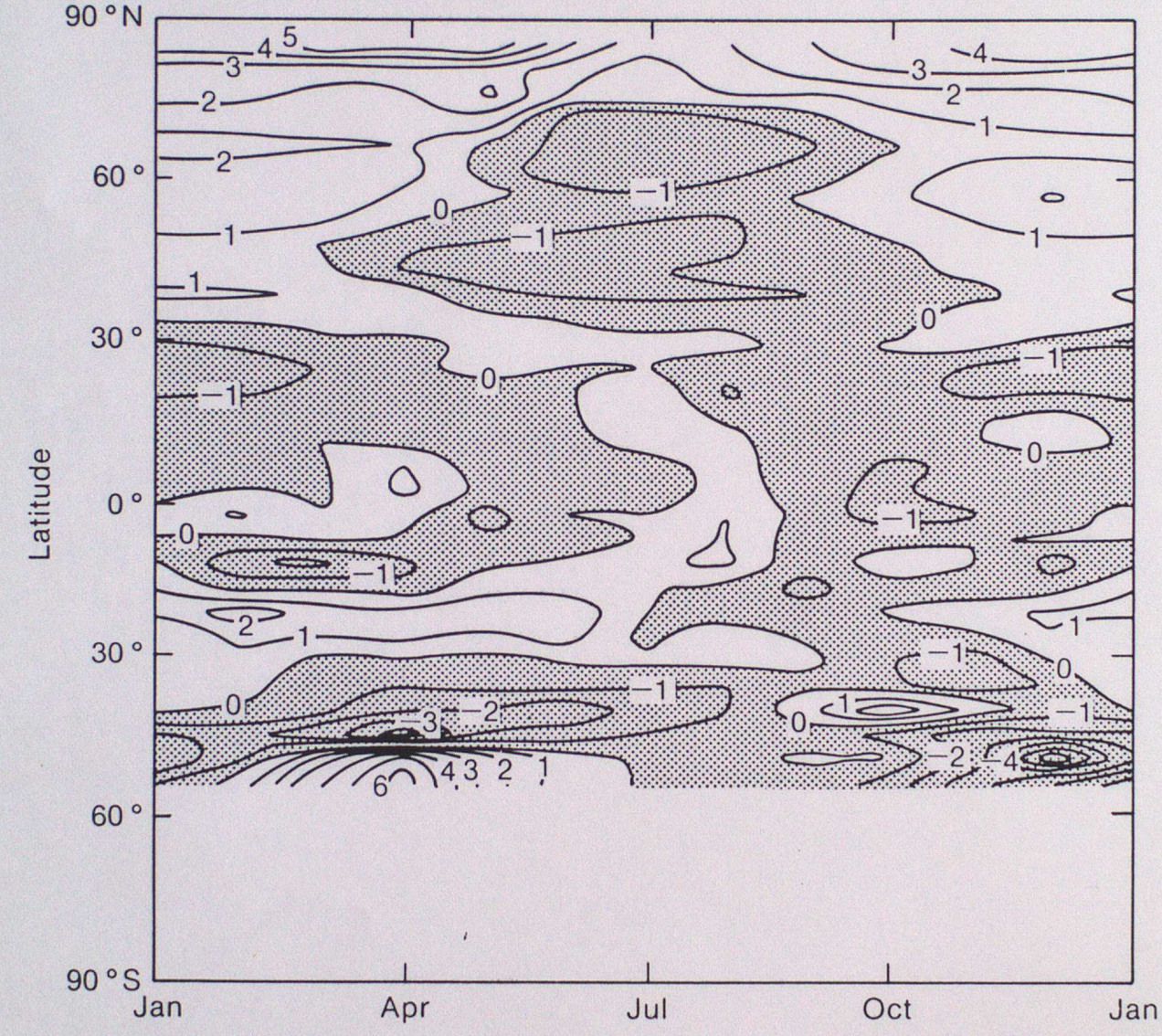

Figure 10

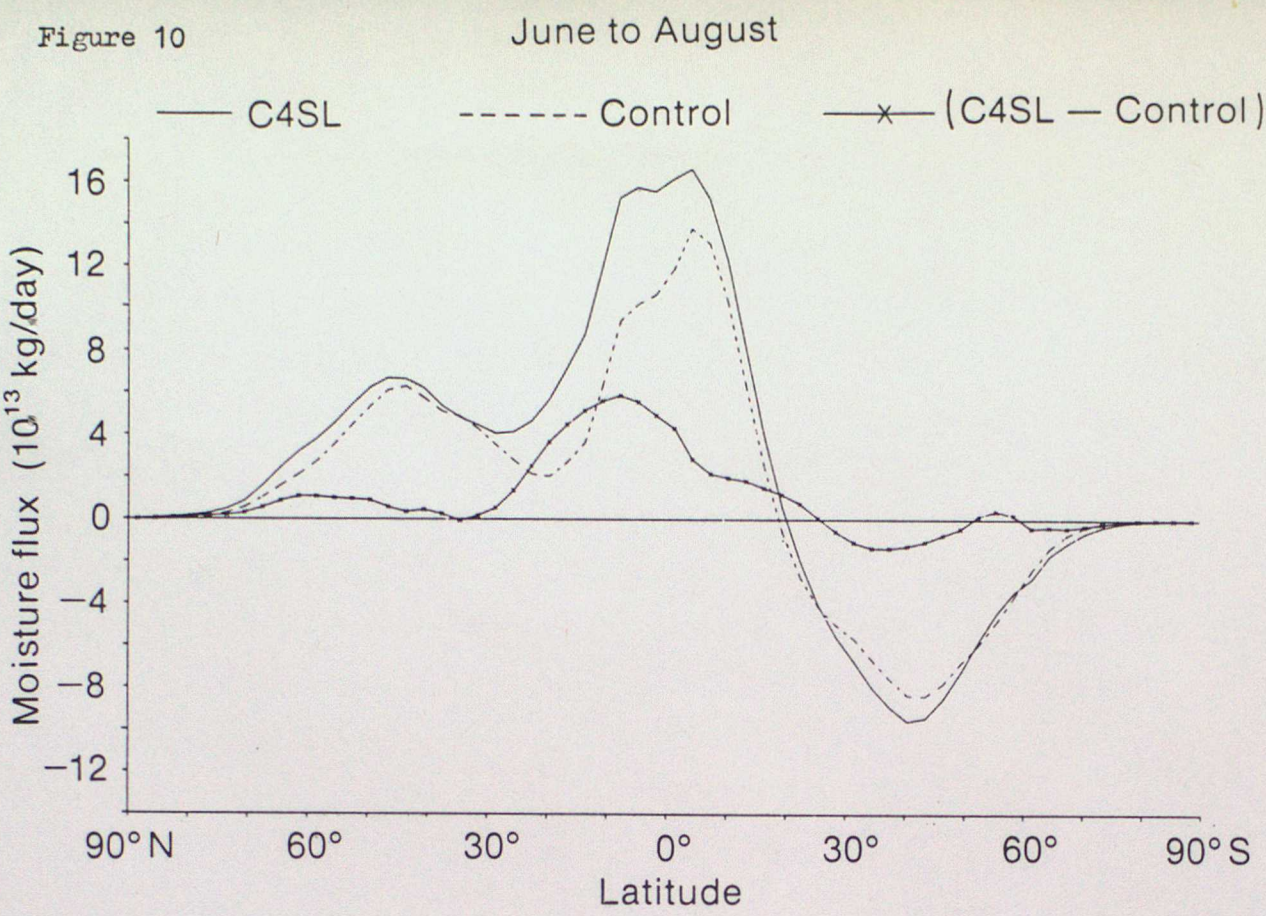
June to August
C4SL
Control
(C4SL — Control)
Moisture flux (10^{13} kg/day)
16
12
8
4
0
−4
−8
−12
90° N
60°
30°
0°
30°
60°
90° S
Latitude

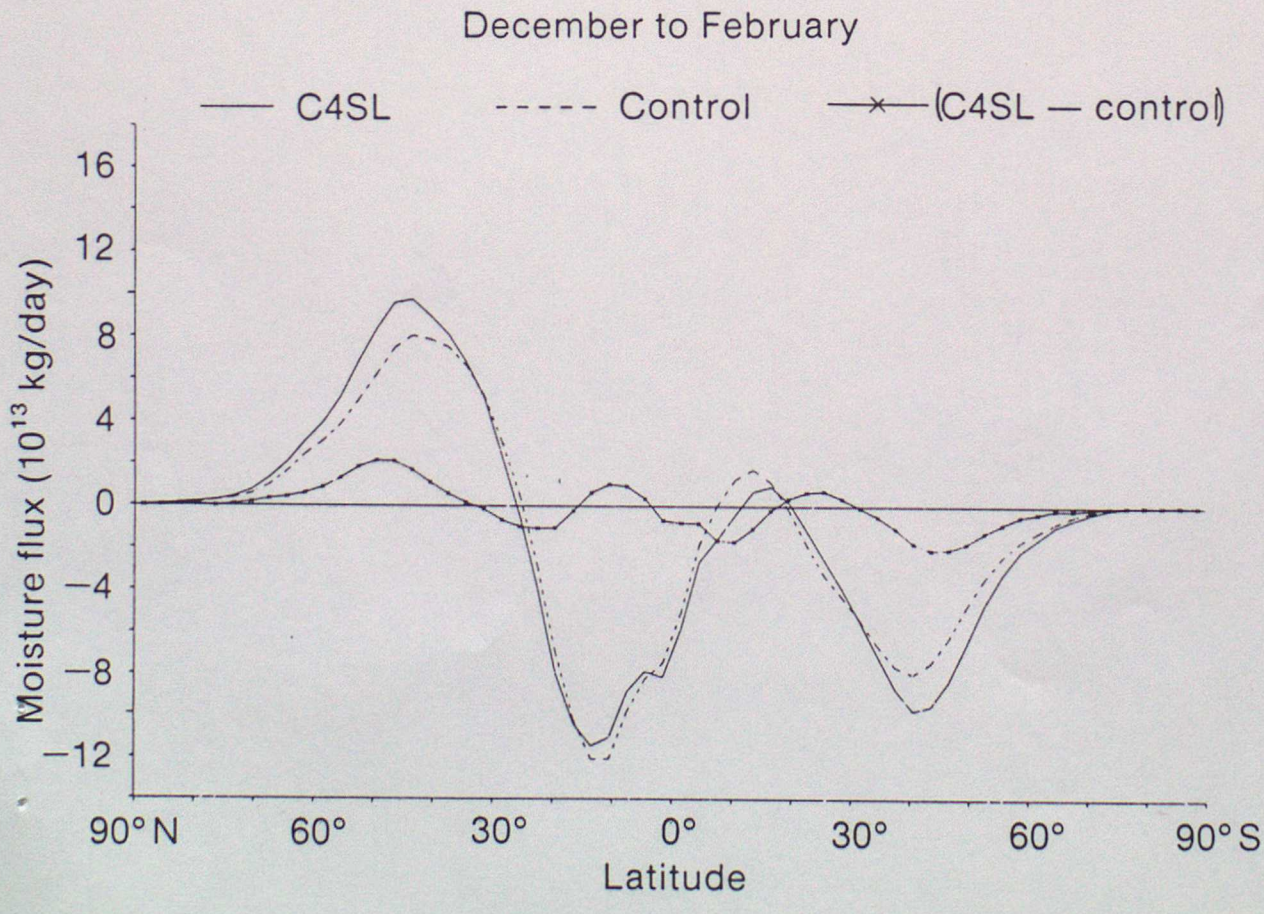
December to February
C4SL
Control
(C4SL — control)
Moisture flux (10^{13} kg/day)
16
12
8
4
0
−4
−8
−12
90° N
60°
30°
0°
30°
60°
90° S
Latitude

FIGURE 11a

CHANGES IN PRECIPITATION DUE TO QUADRUPLING CO_2
AND ENHANCING SSTs (mm/day)
JUNE JULY AUGUST

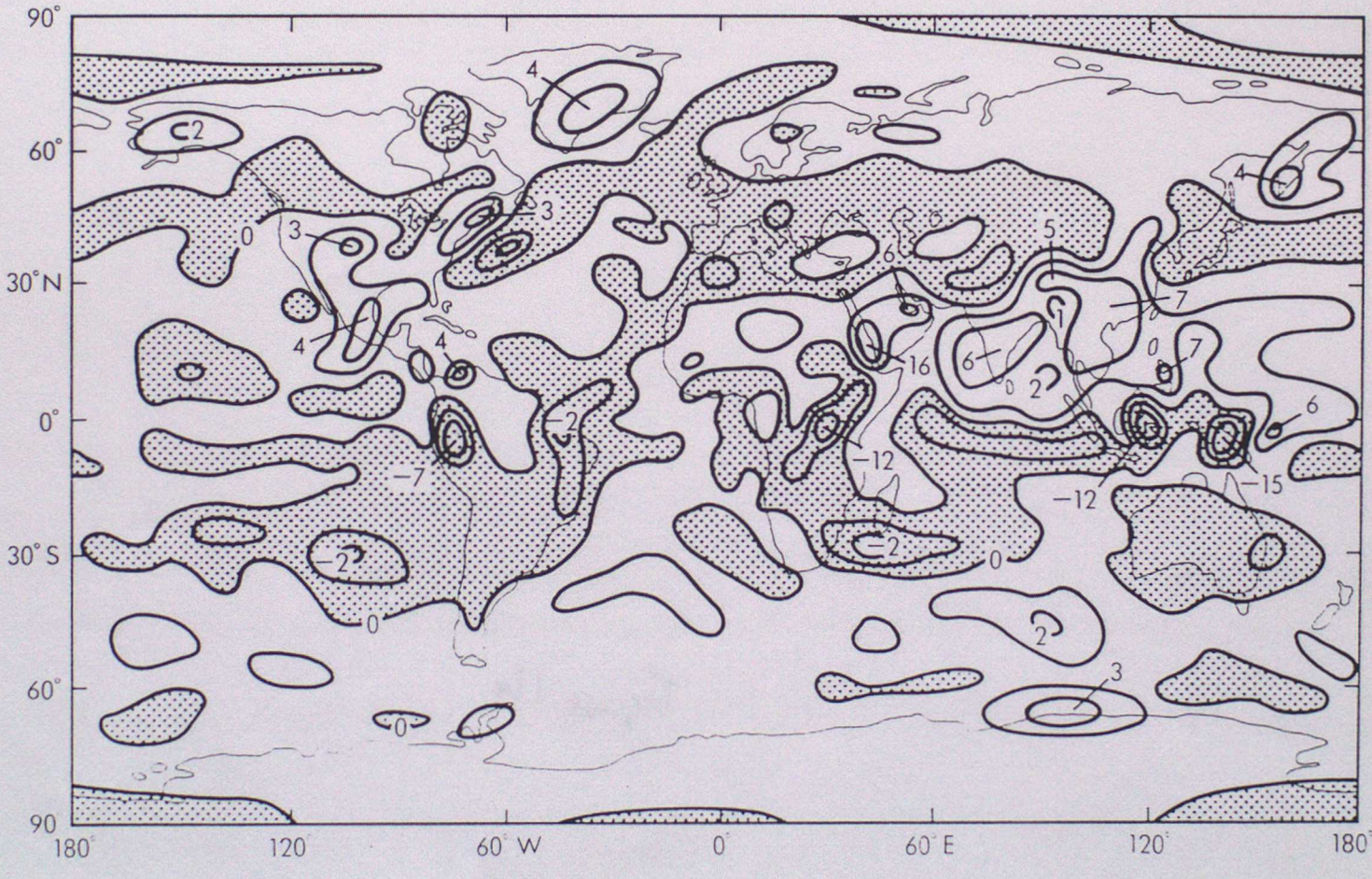

FIGURE 11b

CHANGES IN PRECIPITATION DUE TO QUADRUPLING CO_2
AND ENHANCING SST s (mm/day)
DECEMBER JANUARY FEBRUARY

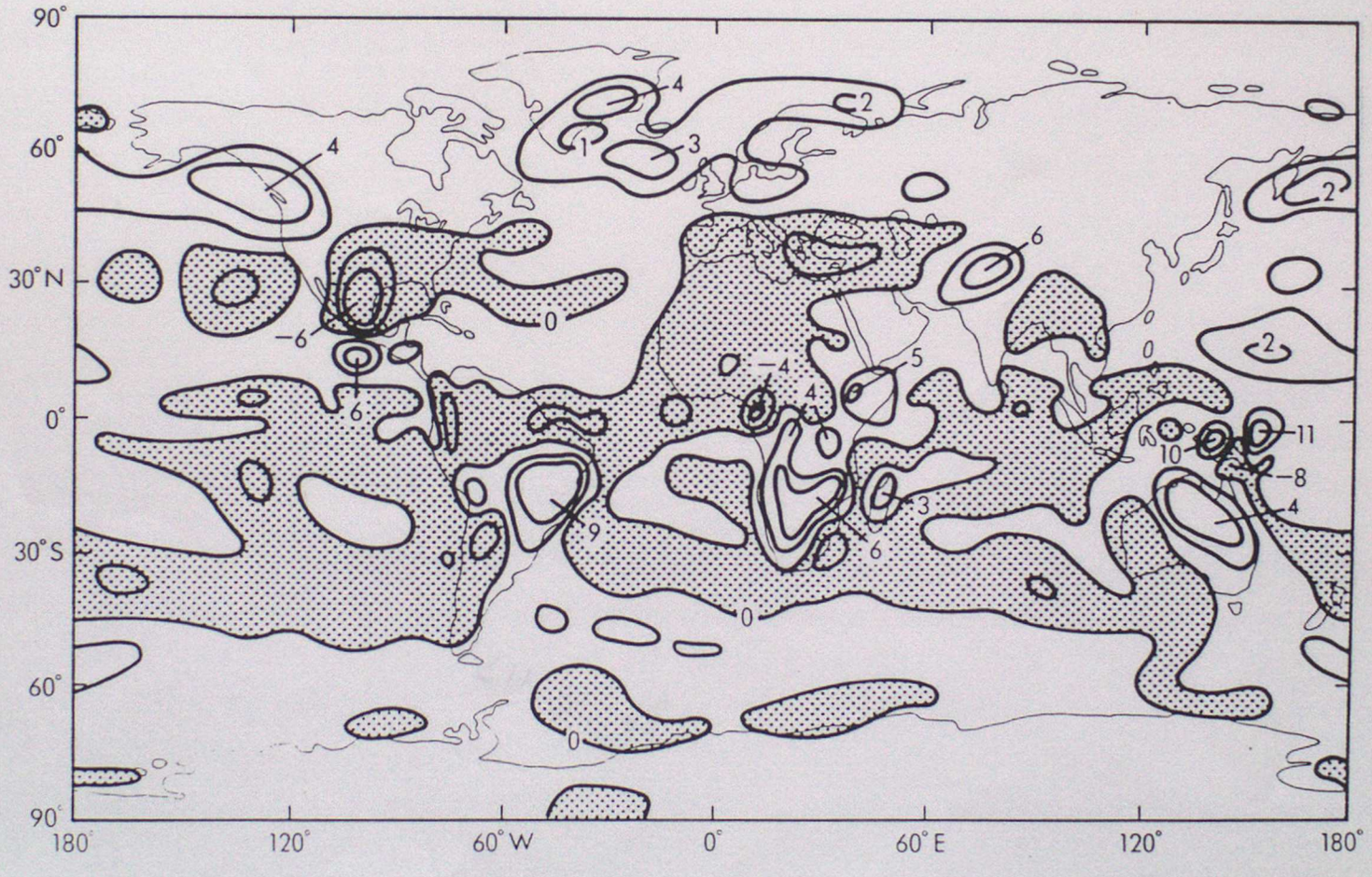

Figure 12

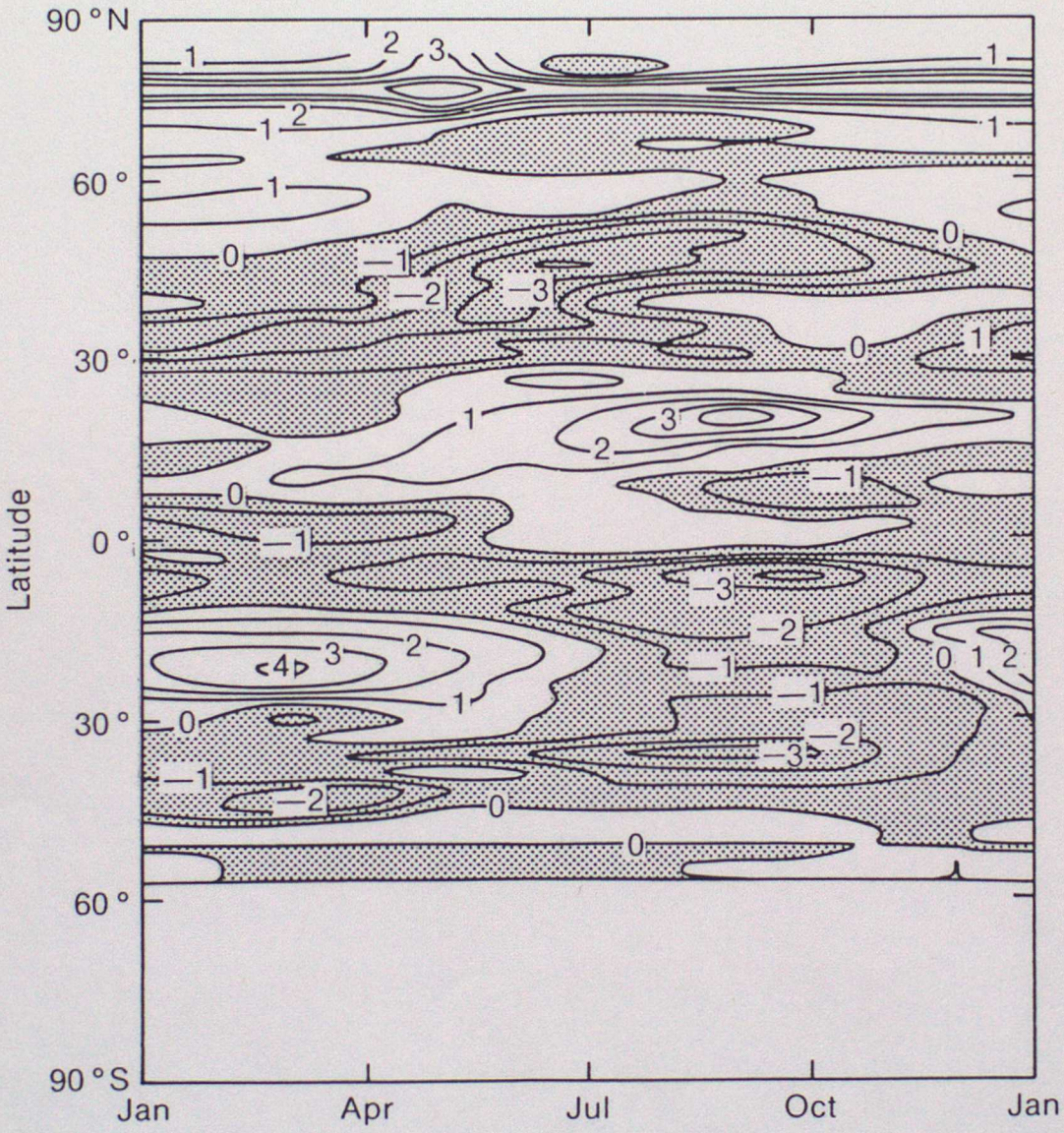

Figure 13

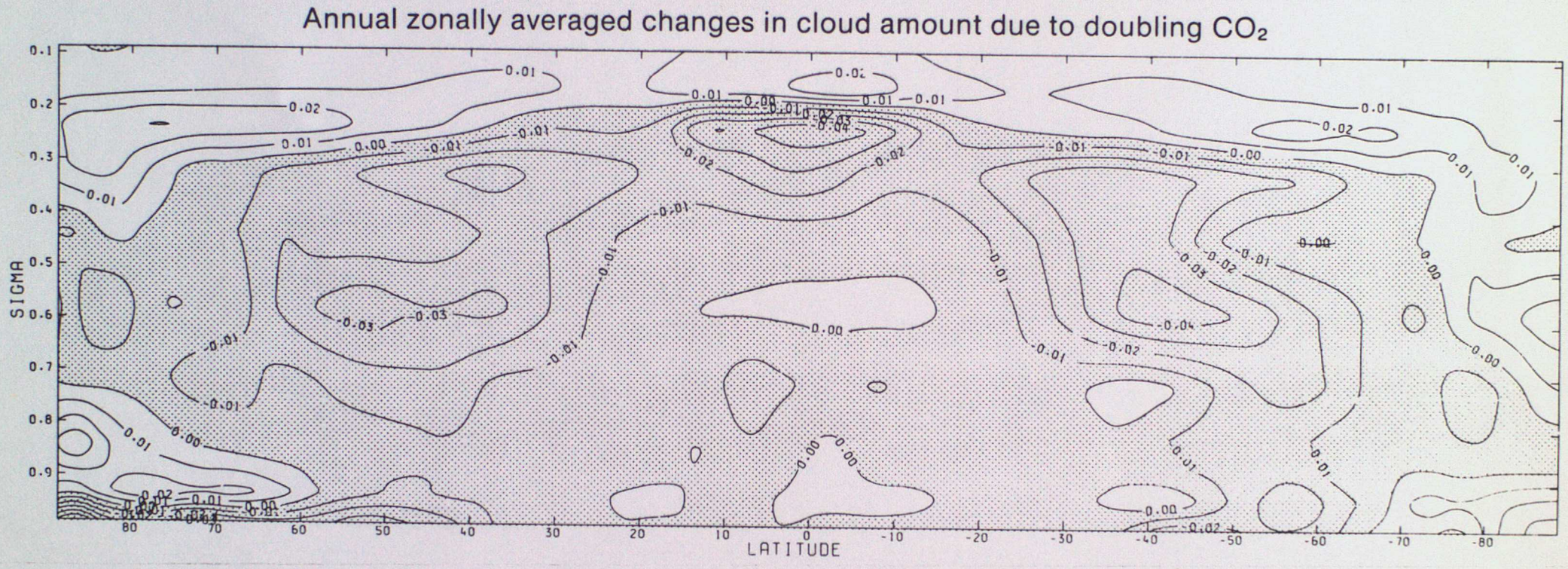
Annual zonally averaged changes in cloud amount due to doubling CO_2
SIGMA
LATITUDE
0.1
0.2
0.3
0.4
0.5
0.6
0.7
0.8
0.9
80
70
60
50
40
30
20
10
0
-10
-20
-30
-40
-50
-60
-70
-80

Figure 14a

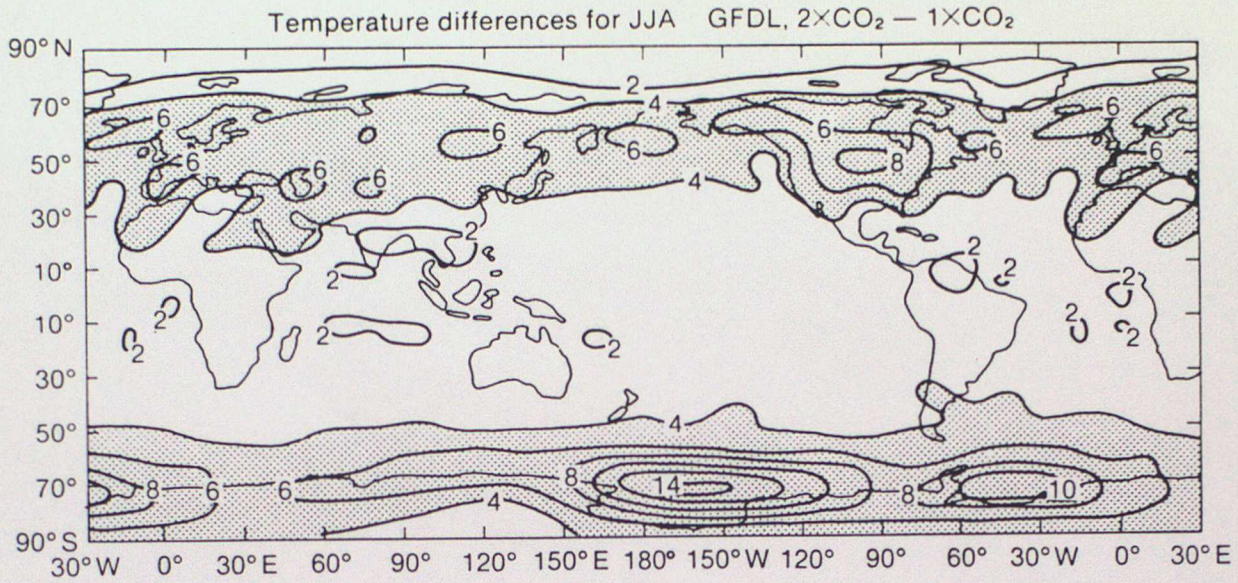

Figure 14b

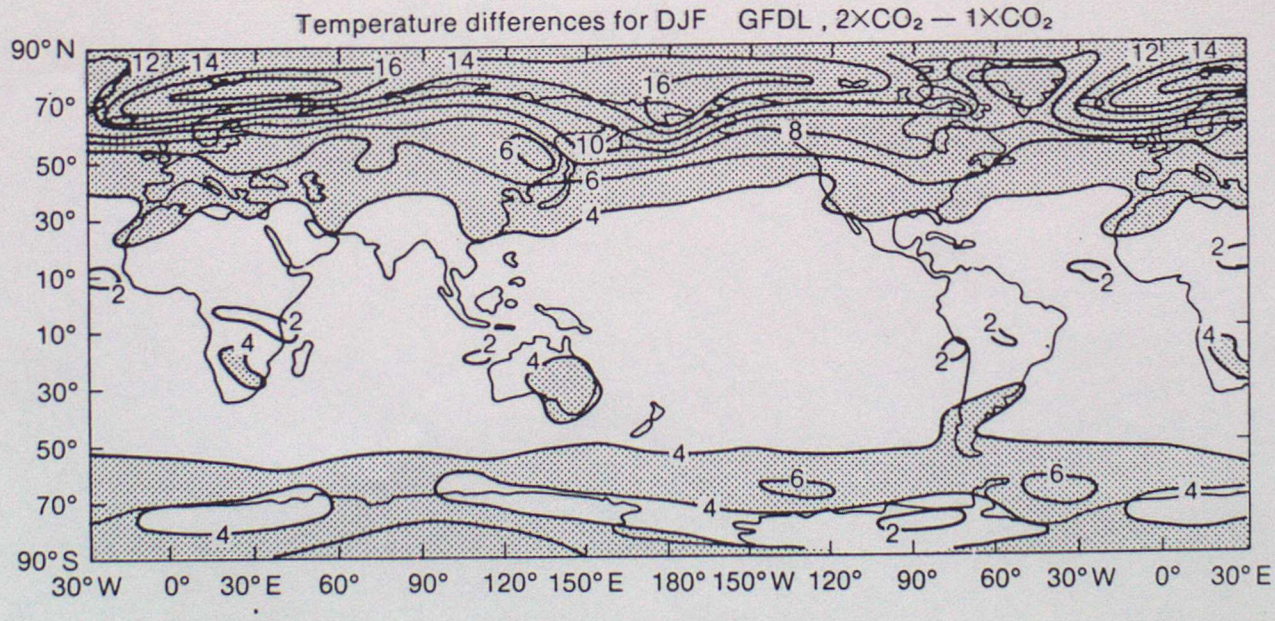

Figure 15

PRECIPITATION DIFFERENCES DEC.JAN.FEB 8 YEAR MEANS
CONTOURS AT 0.+-1.+-2. SHADED WHERE NEGATIVE

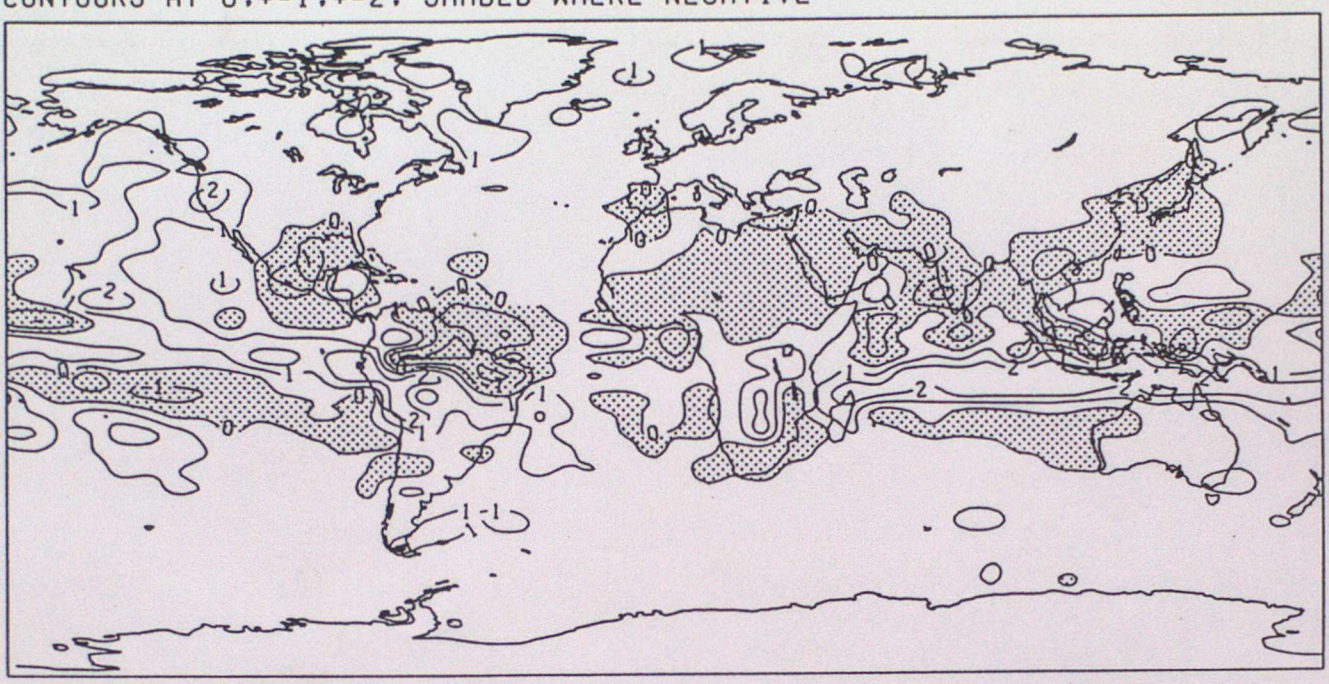

(a)

PRECIPITATION DIFFERENCES JUN.JUL.AUG 8 YEAR MEANS
CONTOURS AT 0.+-1.+-2. SHADED WHERE NEGATIVE

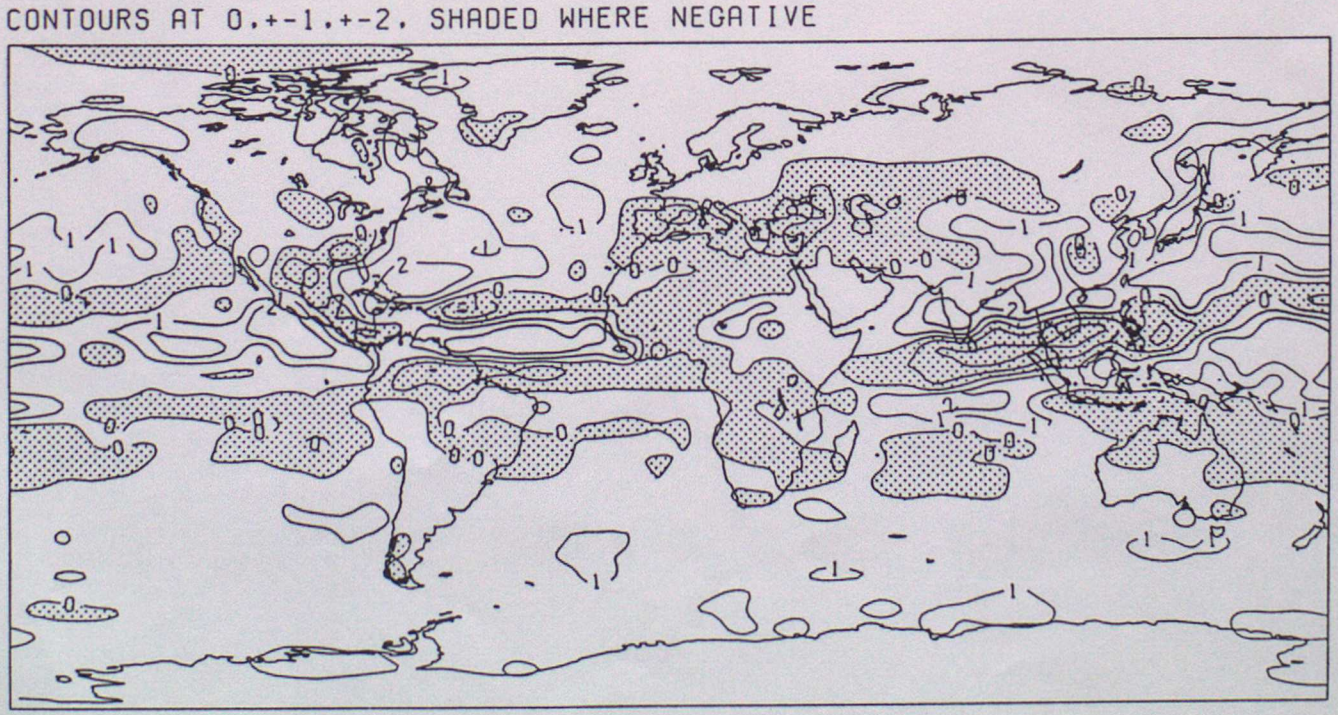

(b)

Figure 16

SOIL MOISTURE DIFFERENCES JUN.JUL.AUG 8 YEAR MEANS
ISOPLETHS AT +/-1, 2, 5 10 AND 15CM. SHADED NEGATIVE

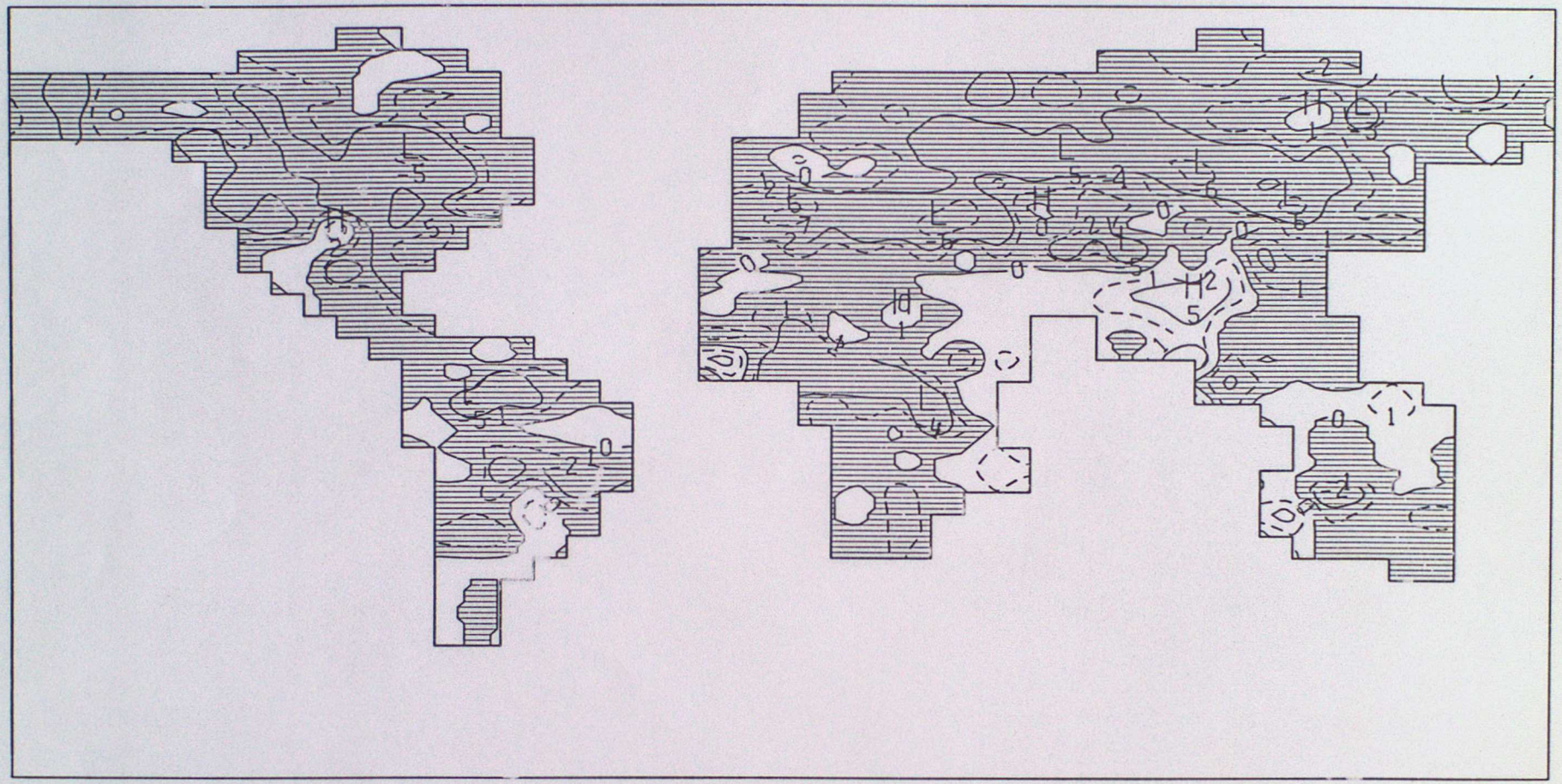

Figure 17

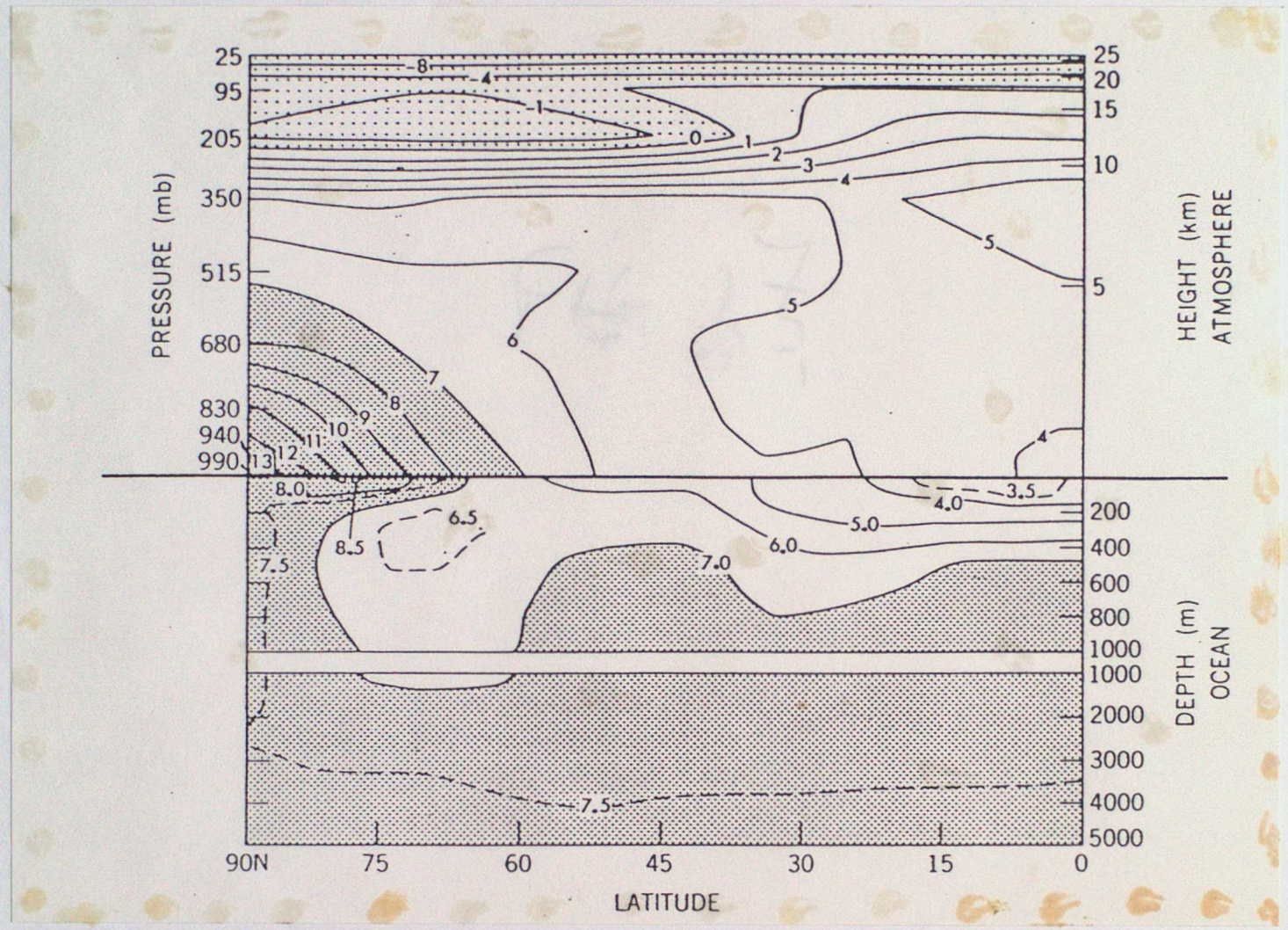
PRESSURE (mb)
25
95
205
350
515
680
830
940
990
HEIGHT (km) ATMOSPHERE
25
20
15
10
5
DEPTH (m) OCEAN
200
400
600
800
1000
1000
2000
3000
4000
5000
90N
75
60
45
30
15
0
LATITUDE
-8
-4
-1
0
1
2
3
4
5
6
7
8
9
10
11
12
13
8.0
8.5
6.5
7.5
7.0
6.0
5.0
4.0
3.5

Figure 18

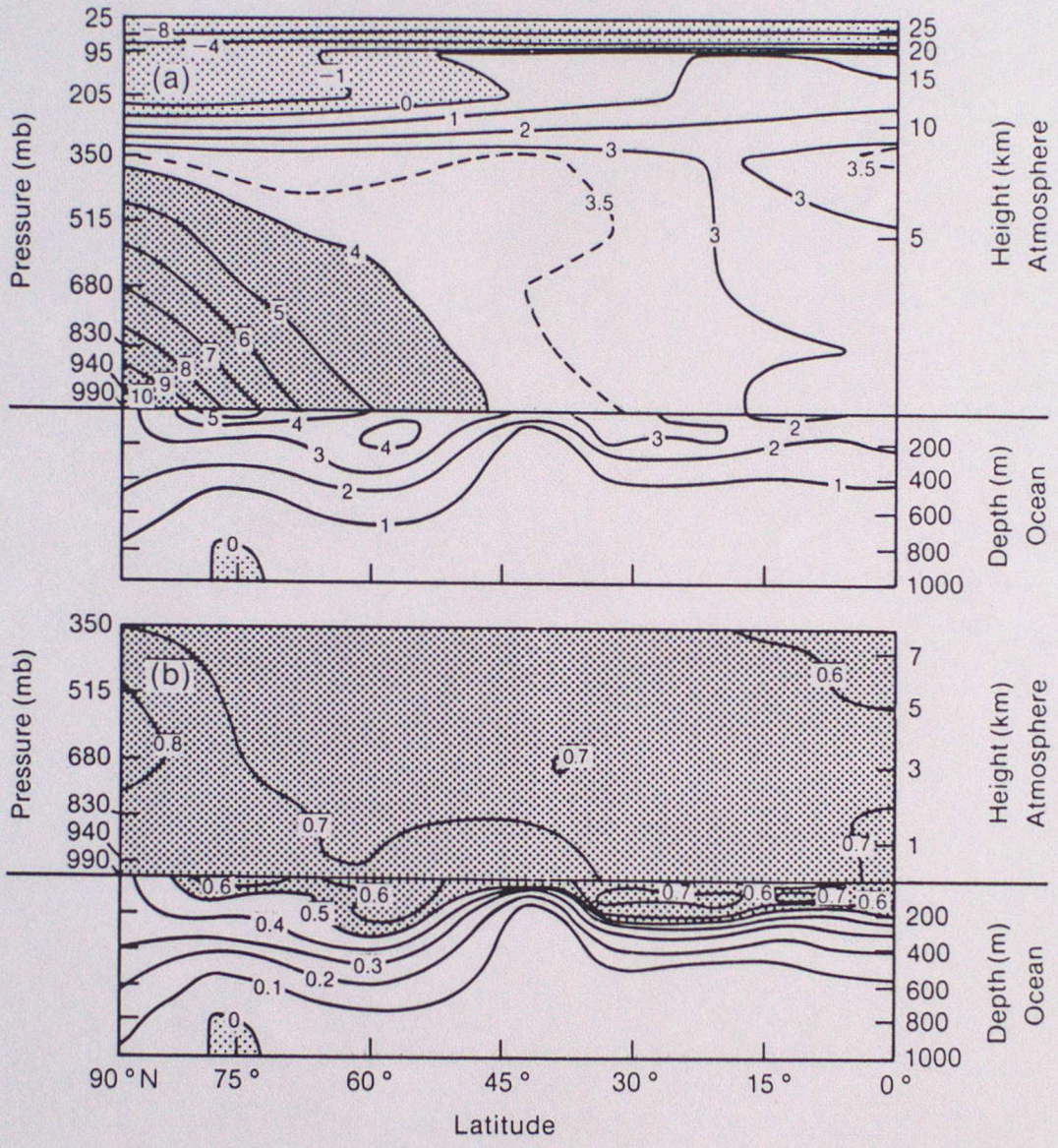
(a)
(b)
Pressure (mb)
25
95
205
350
515
680
830
940
990
Height (km)
Atmosphere
25
20
15
10
5
Depth (m)
Ocean
200
400
600
800
1000
7
5
3
1
90 °N
75 °
60 °
45 °
30 °
15 °
0 °
Latitude

Figure 19

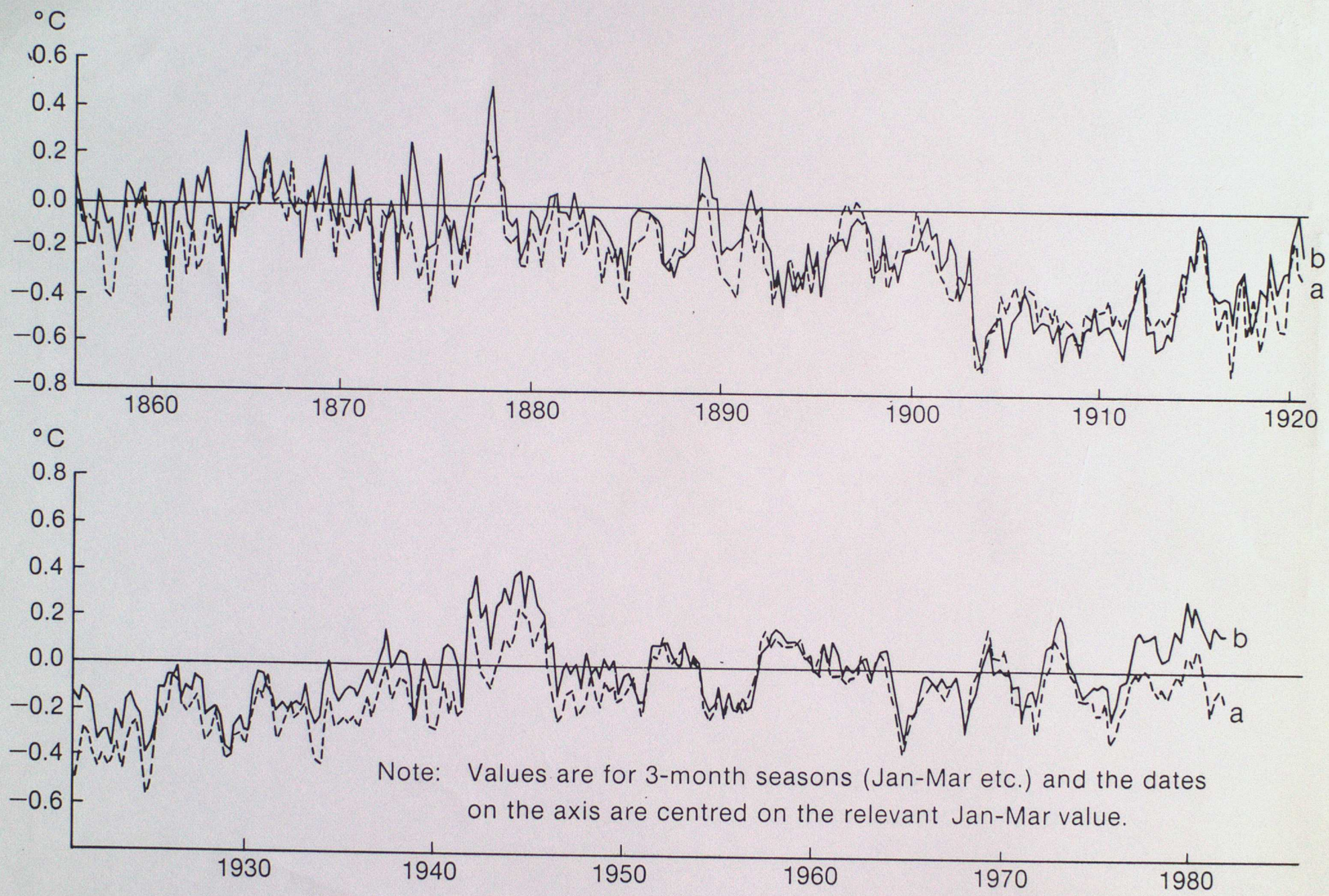

Note: Values are for 3-month seasons (Jan-Mar etc.) and the dates on the axis are centred on the relevant Jan-Mar value.